Measurement of Υ production in pp collisions at $\sqrt{s} = 5\,\mathrm{TeV}$

LHCb collaboration[†]

Abstract

The production cross-sections of Υ mesons, namely $\Upsilon(1S)$, $\Upsilon(2S)$ and $\Upsilon(3S)$, in pp collisions at $\sqrt{s} = 5\,\mathrm{TeV}$ are measured with a data sample corresponding to an integrated luminosity of $9.13 \pm 0.18\,\mathrm{pb}^{-1}$ collected by the LHCb detector. The Υ mesons are reconstructed in the decay mode $\Upsilon \to \mu^+\mu^-$. Double differential cross-sections times branching fractions, as functions of the transverse momentum p_{T} and the rapidity y of the Υ mesons, are measured in the range $p_{\mathrm{T}} < 20\,\mathrm{GeV}/c$ and $2.0 < y < 4.5$. The results integrated over these p_{T} and y ranges are

$$\begin{aligned}
\sigma(\Upsilon(1S)) \times \mathcal{B}(\Upsilon(1S) \to \mu^+\mu^-) &= 2101 \pm 33 \pm 83\,\mathrm{pb}, \\
\sigma(\Upsilon(2S)) \times \mathcal{B}(\Upsilon(2S) \to \mu^+\mu^-) &= 526 \pm 20 \pm 21\,\mathrm{pb}, \\
\sigma(\Upsilon(3S)) \times \mathcal{B}(\Upsilon(3S) \to \mu^+\mu^-) &= 242 \pm 16 \pm 10\,\mathrm{pb},
\end{aligned}$$

where the first uncertainties are statistical and the second are systematic. The ratios of cross-sections between measurements of two different Υ states and between measurements at different centre-of-mass energies are determined. The nuclear modification factor of $\Upsilon(1S)$ at $\sqrt{s} = 5\,\mathrm{TeV}$ is updated as well using the directly measured cross-section results from this analysis.

[†]Authors are listed at the end of this paper.

arXiv:2212.12664v4 [hep-ex] 24 Jul 2023

1 Introduction

The production of heavy quark-antiquark resonances (quarkonia) at hadron colliders provides important information about the strong interaction, which is described by Quantum Chromodynamics (QCD). Based on the assumption of factorization, the production process can be separated into two steps, the generation of a heavy quark pair ($Q\overline{Q}$) through the interaction of partons, and the subsequent hadronization of the quark pair into the quarkonium state. The first step can be calculated within perturbative QCD, while the latter one is nonperturbative and needs to be described by phenomenological models. In the Colour Singlet Model [1–7], the intermediate $Q\overline{Q}$ state is assumed to be colourless, and has the same spin-parity quantum numbers as the final state quarkonium. On the other hand, in the Colour Evaporation Model [4, 8–10], the probability of forming a specific quarkonium state is assumed to be independent of the color of the $Q\overline{Q}$ pair. In the nonrelativistic QCD (NRQCD) approach [11–13], intermediate $Q\overline{Q}$ states with all possible colour-spin-parity quantum numbers may evolve into the desired quarkonium. The transition probabilities, described by long-distance matrix elements (LDMEs) in NRQCD, are nonperturbative and are determined by fitting to experimental data. The LDMEs are assumed to be independent of the production mechanism and kinematics.

Although our understanding of hadronic production of heavy quarkonium has improved significantly owing to four decades of theoretical and experimental efforts, the underlying production mechanism is still not fully understood. For example, models fail to predict both cross-sections and polarisations of the measured S-wave heavy quarkonia states over the entire transverse momentum (p_{T}) and rapidity (y) range [14–16]. Furthermore, model calculations overestimate low-p_{T} (p_{T} less than the $Q\overline{Q}$ invariant mass) cross-sections [14], which dominate the p_{T}-integrated production. The direct measurement of heavy quarkonium cross-sections at different colliding energies is a powerful tool to test production models and provides inputs to studies using heavy ion data [17].

At LHCb, the production of Υ mesons has been studied via the $\mu^+\mu^-$ final state in pp collisions at the centre-of-mass energies of 2.76, 7, 8 and 13 TeV [18–20]. In this analysis, a measurement of the production cross-sections of $\Upsilon(1S)$, $\Upsilon(2S)$ and $\Upsilon(3S)$ is performed, at the centre-of-mass energy of $\sqrt{s} = 5$ TeV. The data are collected by the LHCb detector in 2015 and correspond to an integrated luminosity of $9.13 \pm 0.18\,\mathrm{pb}^{-1}$ [21]. The production cross-sections are measured as functions of the transverse momentum and the rapidity of Υ mesons, in the range $p_{\mathrm{T}} < 20\,\mathrm{GeV}/c$ and $2.0 < y < 4.5$. The result is used to update the nuclear modification factor ($R_{p\mathrm{Pb}}$) reported by LHCb for Υ production in $p\mathrm{Pb}$ collisions at the nucleon-nucleon centre-of-mass energy of $\sqrt{s_{\mathrm{NN}}} = 5$ TeV [17].

2 The LHCb detector and event selection

The LHCb detector [22, 23] is a single-arm forward spectrometer covering the pseudorapidity range $2 < \eta < 5$, designed for the study of particles containing b or c quarks. The detector includes a high-precision tracking system consisting of a silicon-strip vertex detector surrounding the pp interaction region [24], a large-area silicon-strip detector located upstream of a dipole magnet with a bending power of about $4\,\mathrm{Tm}$, and three stations of silicon-strip detectors and straw drift tubes [25] placed downstream of the magnet. The tracking system provides a measurement of the momentum, p, of charged

particles with a relative uncertainty that varies from 0.5% at low momentum to 1.0% at $200\,\mathrm{GeV}/c$. Muons are identified by a system composed of alternating layers of iron and multiwire proportional chambers [26].

The online event selection is performed by a trigger [27], which consists of a hardware stage selecting events with at least one muon candidate with $p_{\mathrm{T}} > 0.9\,\mathrm{GeV}/c$ based on information from the muon systems, followed by a two-stage software stage, which applies a full event reconstruction. In the software trigger, two muon candidates, each having $p_{\mathrm{T}} > 0.5\,\mathrm{GeV}/c$ and $p > 3\,\mathrm{GeV}/c$, are required to form a good quality vertex with invariant mass $m(\mu^+\mu^-) > 4.7\,\mathrm{GeV}/c^2$. In between the two software stages, an alignment and calibration of the detector is performed in near real-time and their results are used in the second stage of the trigger [28]. The same alignment and calibration information is propagated to the offline reconstruction, ensuring consistent and high-quality particle identification (PID) information between the trigger and offline software. The identical performance of the online and offline reconstruction offers the opportunity to perform physics analyses directly using candidates reconstructed in the trigger [27, 29], which the present analysis exploits.

Candidate Υ mesons are further selected offline, where two muon tracks are required to have $p_{\mathrm{T}} > 0.65\,\mathrm{GeV}/c$, $p > 10\,\mathrm{GeV}/c$ and $1.9 < \eta < 4.9$, and the invariant mass of the two muons is required to be in the range of $9.0 < m(\mu^+\mu^-) < 10.7\,\mathrm{GeV}/c^2$.

Simulation is required to model the effects of the detector acceptance and the imposed selection requirements. In the simulation, pp collisions are generated using PYTHIA [30] with a specific LHCb configuration [31]. Decays of unstable particles are described by EVTGEN [32], in which final-state radiation is generated using PHOTOS [33]. The interaction of the generated particles with the detector, and its response, are implemented using the GEANT4 toolkit [34] as described in Ref. [35].

3   Cross-section determination

The double-differential cross-section times the $\Upsilon \to \mu^+\mu^-$ branching fraction ($\mathcal{B}$) of Υ production in a given (p_{T}, y) bin is defined as

$$\mathcal{B}(\Upsilon \to \mu^+\mu^-) \times \frac{\mathrm{d}^2\sigma}{\mathrm{d}p_T\mathrm{d}y} = \frac{N(\Upsilon \to \mu^+\mu^-)}{\mathcal{L} \times \varepsilon_{\mathrm{tot}} \times \Delta p_T \times \Delta y}, \tag{1}$$

where $N(\Upsilon \to \mu^+\mu^-)$ is the yield of $\Upsilon \to \mu^+\mu^-$ signal decays, $\varepsilon_{\mathrm{tot}}$ is the total efficiency in a (p_{T}, y) bin, $\mathcal{L}$ is the integrated luminosity, and Δp_{T} and Δy are the interval widths of the Υ transverse momentum and rapidity, respectively.

The Υ yield in each (p_{T}, y) bin is determined with an extended unbinned maximum-likelihood fit to the invariant-mass distribution of the Υ candidates, denoted as m_Υ in the following. Four components are used to describe the distributions, the three Υ signals and a combinatorial background. The mass distribution for each of the $\Upsilon(1S)$, $\Upsilon(2S)$ and $\Upsilon(3S)$ states is described by a Crystal Ball (CB) function [36]. The differences between the means and the ratios of the widths of these CB functions are fixed, respectively, to the differences and the ratios of the world-average $\Upsilon(nS)$ masses [37]. The CB function parameters α and n, which describe the radiative tail of the Υ mass distribution, are fixed to the values of $\alpha = 2$ and $n = 1$, following the same approach of the previous

analyses [19, 20]. The mass distribution of the combinatorial background contribution is described by an exponential function.

The invariant mass distribution of all candidates for $p_{\mathrm{T}} \in [0, 20]\,\mathrm{GeV}/c$ and $y \in [2.0, 4.5]$ is shown in Fig. 1, with the fit result superimposed. The yields of $\Upsilon(1S)$, $\Upsilon(2S)$ and $\Upsilon(3S)$ signals are 7560 ± 120, 1900 ± 70 and 930 ± 60, respectively.
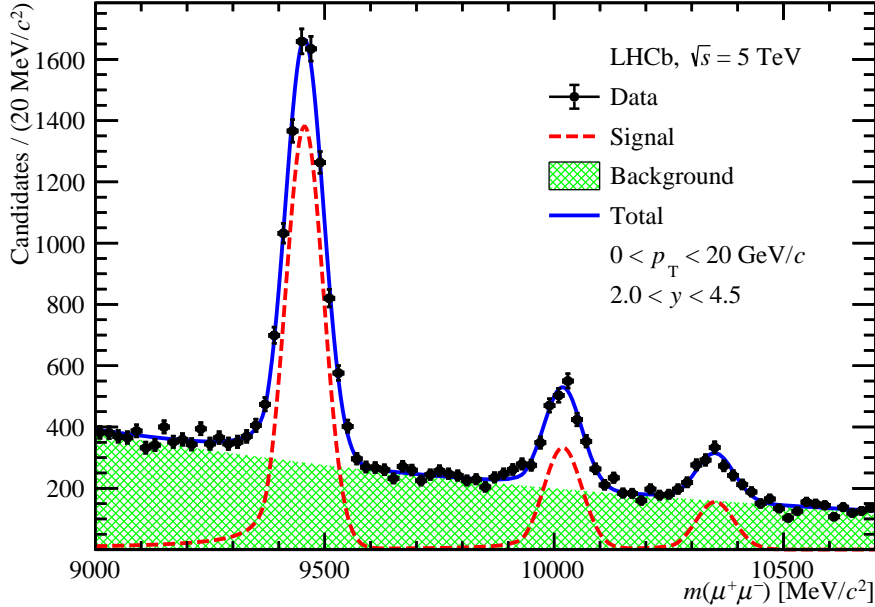

Figure 1: Invariant mass distribution of Υ candidates in the kinematic range $p_{\mathrm{T}} \in [0, 20]\,\mathrm{GeV}/c$ and $y \in [2.0, 4.5]$. The result of the fit with three Crystal Ball functions for the signal plus an exponential function for the background is also shown.

The total efficiency $\varepsilon_{\mathrm{tot}}$ is expressed as the product of four components: the geometrical acceptance, ϵ_{Acc}, the reconstruction and selection efficiency, $\epsilon_{\mathrm{Rec\&Sel}}$, the muon identification efficiency, ϵ_{PID}, and the trigger efficiency, ϵ_{Trg}, as

$$\varepsilon_{\mathrm{tot}} = \epsilon_{\mathrm{Acc}} \times \epsilon_{\mathrm{Rec\&Sel}} \times \epsilon_{\mathrm{Pid}} \times \epsilon_{\mathrm{Trg}}. \tag{2}$$

These efficiencies in general depend on the Υ polarisation. The measurement of the Υ polarisation by LHCb at $\sqrt{s} = 7$ and $8\,\mathrm{TeV}$ [38] in pp collisions indicates that the three polarisation parameters λ_{θ}, $\lambda_{\theta\phi}$ and λ_{ϕ} are consistent with zero. Therefore, the efficiencies are determined in each (p_{T}, y) bin for the $\Upsilon(1S)$, $\Upsilon(2S)$ and $\Upsilon(3S)$ mesons, assuming the Υ states are unpolarised. Variations of cross-sections due to polarisation are studied for different scenarios of the polarisation parameter λ_{θ}, as the dependence of the efficiency on the $\lambda_{\theta\phi}$ and λ_{ϕ} parameters is smaller [39].

The quantity ϵ_{Acc} is calculated using the simulation sample without a prior geometrical acceptance requirement on the muons. The efficiency $\epsilon_{\mathrm{Rec\&Sel}}$ is determined using full simulation samples for which the distributions of charged track multiplicity of pp collisions and Υ rapidity are corrected to match data. The efficiency ϵ_{PID} is calculated using the single muon PID efficiency in bins of (p, η) weighted by the muon (p, η) distribution in simulation samples. The single-muon PID efficiency is obtained using $J/\psi \to \mu^+ \mu^-$ decays in calibration data [40, 41]. The efficiency ϵ_{Trg} is determined on simulated events.

3

4 Systematic uncertainties

Several sources of systematic uncertainty are expected to affect the cross-section measurements: determination of the signal yields, efficiency calculations and computation of the integrated luminosity. The efficiency-related uncertainties are determined with independent simulation samples for each $\Upsilon(nS)$ meson, and are expected to be similar for the three states. They are reported in Table 1 and discussed in detail in the following. The total uncertainty is calculated as the quadrature sum of these uncertainties.

Table 1: Relative systematic uncertainty (%) from various sources. The ranges correspond to results measured in each (p_T, y) bin of Υ mesons. For some systematic uncertainties, the results are correlated among different (p_T, y) bins as noted in the last column.

	Source	$\Upsilon(1S)$	$\Upsilon(2S)$	$\Upsilon(3S)$	Comment
Signal yields	Fit model	2.5	2.8	3.1	Correlated
Efficiency ϵ	Trigger	0.7–1.9	0.7–2.1	0.7–1.9	Correlated
	Track reconstruction	1.7–3.1	1.7–3.2	1.7–3.4	Correlated
	MuonID	0.5–5.3	0.5–5.1	0.5–5.2	Correlated
	Kinematic spectrum	0.0–4.9	0.0–4.5	0.0–6.3	Uncorrelated
	Final-state radiation	1.0	1.0	1.0	Correlated
	Simulation sample size	0.5–4.5	0.4–3.3	0.4–3.4	Uncorrelated
Luminosity		2.0	2.0	2.0	Correlated

The systematic uncertainty from the determination of the signal yields is affected by the invariant-mass fit model and is estimated using pseudoexperiments. The pseudoexperiments employ a mixture of $\Upsilon(1S)$ signal in the full simulation sample and background generated according to the background model fitted in data. In the pseudoexperiments, the relative fraction of the two components is chosen such that the level of background matches the data in the Υ signal region. This signal-plus-background sample is fitted with the same model as for the data. The systematic uncertainty is estimated as the relative difference between the signal yield obtained from the fit and that of the input. This study is repeated for the $\Upsilon(1S)$, $\Upsilon(2S)$ and $\Upsilon(3S)$ states, with different fractions of background, yielding 2.5%, 2.8% and 3.1% as the systematic uncertainty for the three states, respectively. The small difference between the uncertainties for the three states is attributed to different background levels under each signal peak.

Systematic uncertainties on both hardware and software trigger efficiency are studied in this analysis. To validate systematic effects on the hardware trigger, the trigger efficiency is determined for μ^+ and μ^- individually and is then used to calculate the efficiency for Υ signals following the method described in Ref. [42]. The difference between the trigger efficiencies obtained on data and simulation is quoted as the systematic uncertainty on the hardware-trigger efficiency. The systematic uncertainty, estimated to be in the range 0.0–1.9%, depends on the (p_T, y) bin of the Υ mesons and is assumed to be correlated among the bins. For the software trigger, alternative efficiency values are determined using a subset of events triggered independently of the Υ signals [43]. Within this sample, the fraction of Υ signal events that passes the software requirement is quoted as the trigger efficiency. The efficiency is calculated for both data and simulation samples in (p_T, y) bins of the Υ mesons, and their difference is taken as the systematic uncertainty.

The track reconstruction efficiency is evaluated for each muon using calibrated simulation and data samples [44], and their difference is used to correct the $\epsilon_{\text{Rec\&Sel}}$ efficiency of simulated Υ decays. A systematic uncertainty of 0.8% per track is assigned to account for the dependency of the correction on the event multiplicity variable that is used to weight simulation to match data. Furthermore, an uncertainty is associated with the correction due to the limited size of the calibration samples, which is propagated to the Υ cross-section measurement using a large number of pseudoexperiments.

The muon identification efficiency is affected by the statistical fluctuation of the PID calibration constants originating from the limited size of calibration samples and from the choice of the (p, η) binning scheme for muons. The statistical uncertainties in the PID efficiencies are propagated to the Υ cross-sections using pseudoexperiments. The variation is found to be below 1% and is therefore neglected. The systematic uncertainty due to the kinematic binning scheme of the calibration sample is studied by measuring the PID efficiency using alternative binning schemes. The difference between the alternative efficiency and the default one is quoted as the systematic uncertainty.

The kinematic distributions of the Υ mesons in data and simulation samples could be different, which may cause a mis-modelling in the underlying detection efficiency. Efficiencies measured in (p_{T}, y) intervals help to reduce the discrepancy, however the (p_{T}, y) bin size can cause systematic effects in the efficiency determination. To check for possible residual effects, the y distributions of the Υ states in simulation are reweighted to match those in data, for which the background has been subtracted using the *sPlot* technique [45]. In this analysis, the y distribution is studied as the efficiencies are found to have only a weak dependence on the p_{T} of the Υ candidates. All the efficiencies are re-calculated with the reweighted y spectrum in the simulation sample, and relative differences between the new results and the default are taken as systematic uncertainties.

Due to the missing energy caused by final-state radiation that is not reconstructed, some signal events are removed by the requirement on the $\mu^+\mu^-$ invariant mass. The efficiency of this requirement is studied using simulation samples. A systematic uncertainty of 1.0% is assigned to take into account possible differences between data and simulated Υ decays, following the method of Ref. [20].

The limited size of the simulation samples used to determine the efficiencies is a source of systematic uncertainty. The relative statistical uncertainties in the efficiencies are propagated to the cross-section measurements. The integrated luminosity has a relative uncertainty of 2.0% [21], which is propagated to the final results as a systematic uncertainty.

5 Results

5.1 Cross-sections

The double-differential cross-sections times the branching fraction of $\Upsilon \to \mu^+\mu^-$ are shown in Fig. 2 and the numeric results are listed in Tables 1, 2 and 3 in Appendix A for $\Upsilon(1S)$, $\Upsilon(2S)$ and $\Upsilon(3S)$, respectively. The cross-section times branching fraction as a function of p_{T} and integrated over y or vice-versa are shown in Fig. 3, and listed in Tables 4 and 5 in Appendix A for the three Υ states. The change of Υ cross-sections for alternative polarisation relative to the zero polarisation is studied for $\lambda_\theta = -1, 0.1$ and $+1$ in the

helicity frame, which is reported in Appendix B. The result for $\lambda_\theta = \pm 1$ corresponds to the extreme transverse and longitudinal polarisation and $\lambda_\theta = 0.1$ is the approximation of LHCb measurement [38]. Results for other λ_θ values can be interpolated.
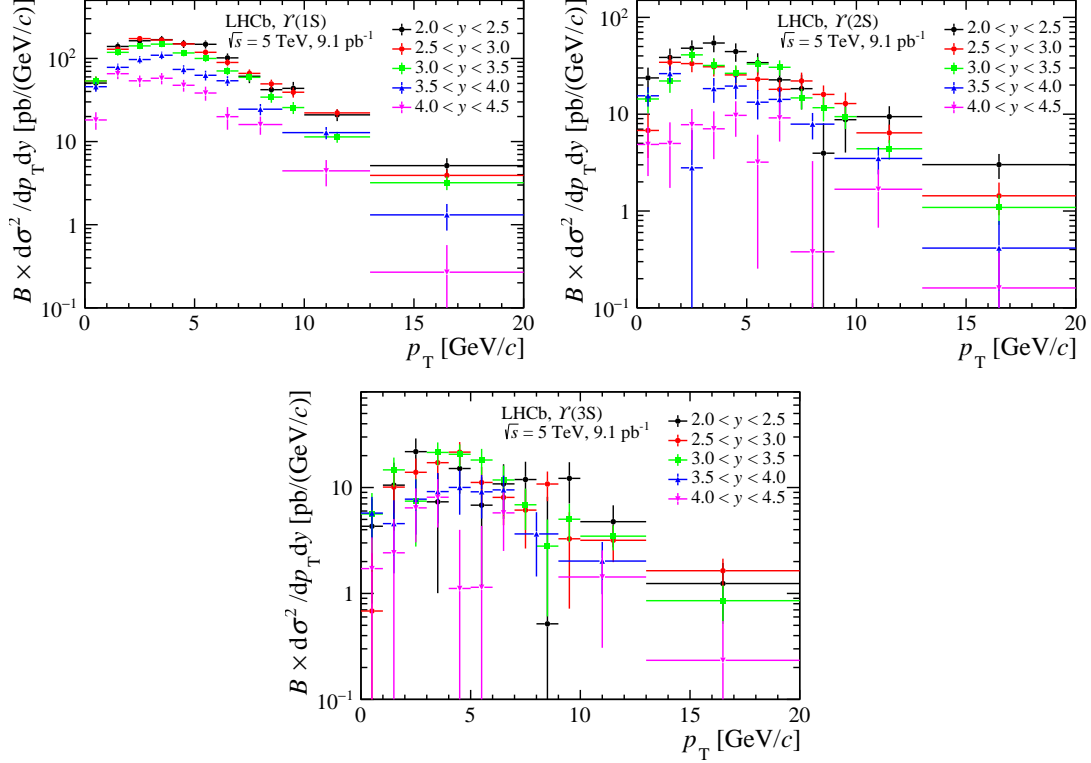

Figure 2: Double-differential cross-section times $\Upsilon \to \mu^+\mu^-$ branching fraction as a function of p_T in bins of y for (upper left) $\Upsilon(1S)$, (upper right) $\Upsilon(2S)$ and (bottom) $\Upsilon(3S)$ mesons. Statistical and systematic uncertainties are added in quadrature.

The differential cross-section times branching fraction as a function of p_T for $\Upsilon(1S)$ mesons for y integrated over 2.0–4.5 are compared with the NRQCD predictions [46] in Fig. 4. The data points are plotted at the mean p_T of each bin. Good agreement is observed between NRQCD predictions and the measurement of this analysis for $p_T > 5 \,\mathrm{GeV}/c$. Another NRQCD calculation that tends to describe high-p_T data at rapidity $y \sim 0$ is found to overestimate the LHCb result [47]. The difference between the two NRQCD calculations is due to different values of LDMEs used in their analyses.

The double-differential cross-sections integrated over the kinematic range of $p_T < 20 \,\mathrm{GeV}/c$ and $2.0 < y < 4.5$ are

$$
\begin{aligned}
\sigma(\Upsilon(1S)) \times \mathcal{B}(\Upsilon(1S) \to \mu^+\mu^-) &= 2101 \pm 33 \,(\text{stat}) \pm 83 \,(\text{syst})\,\text{pb}, \\
\sigma(\Upsilon(2S)) \times \mathcal{B}(\Upsilon(2S) \to \mu^+\mu^-) &= 526 \pm 20 \,(\text{stat}) \pm 21 \,(\text{syst})\,\text{pb}, \\
\sigma(\Upsilon(3S)) \times \mathcal{B}(\Upsilon(3S) \to \mu^+\mu^-) &= 242 \pm 16 \,(\text{stat}) \pm 10 \,(\text{syst})\,\text{pb}.
\end{aligned}
$$

The total cross-section in the LHCb acceptance as a function of pp centre-of-mass energy is shown in Fig. 5 for $\Upsilon(1S)$, $\Upsilon(2S)$ and $\Upsilon(3S)$ mesons. All three distributions show approximately a linear rise as a function of $\sqrt{s}$ in the range 2.76–13 TeV.
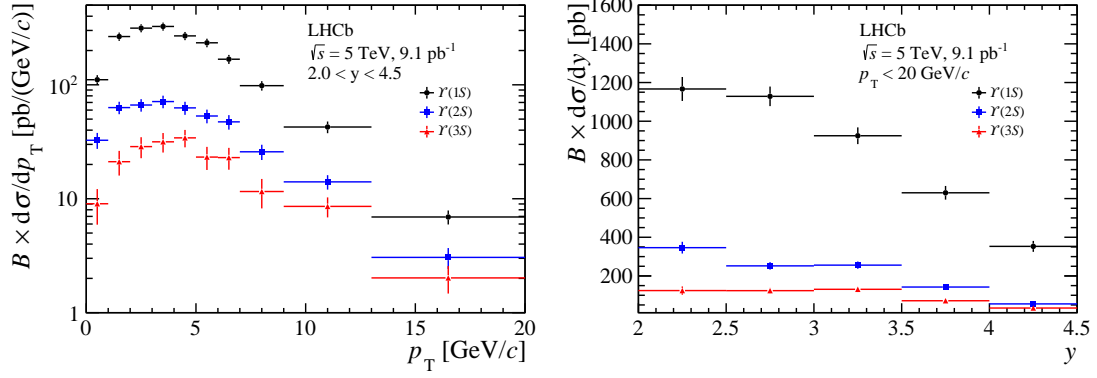
Figure 3: Differential cross-section times $\Upsilon \to \mu^+\mu^-$ branching fraction (left) as a function of p_T for y integrated from 2.0 to 4.5 and (right) as a function of y for p_T integrated from 0 to 20 GeV/c, for the $\Upsilon(1S)$, $\Upsilon(2S)$ and $\Upsilon(3S)$ states. Statistical and systematic uncertainties are added in quadrature.
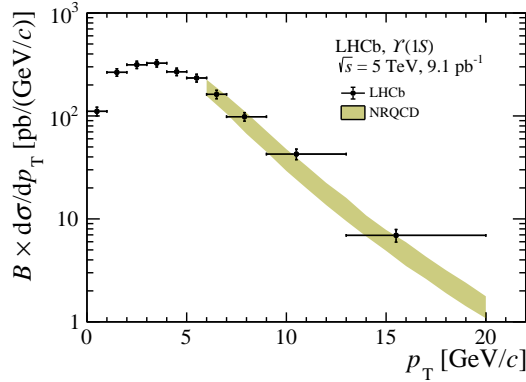
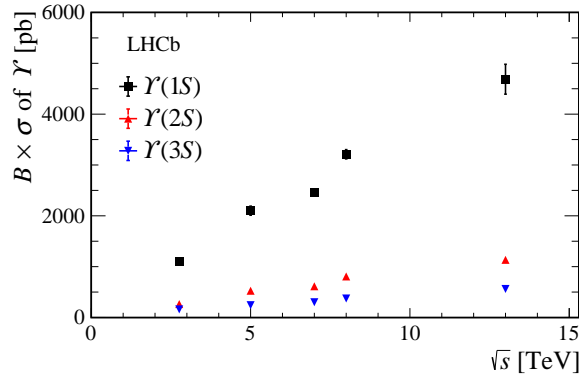Figure 4: Differential cross-section of $\Upsilon(1S)$ mesons as a function of p_T, compared with the NRQCD prediction of Ref. [46].

Figure 5: Production cross-sections in the range $p_T < 15$ GeV/c and $2.0 < y < 4.5$ multiplied by $\Upsilon \to \mu^+\mu^-$ branching fractions as a function of the centre-of-mass energy of pp collisions for (black boxes) $\Upsilon(1S)$, (red upward triangles) $\Upsilon(2S)$ and (blue downward triangles) $\Upsilon(3S)$ states. Statistical and systematic uncertainties are added in quadrature.

7

5.2 Cross-section ratios

The cross-section ratios between the different Υ states are calculated as:

$$R_{2S/1S} \equiv \frac{\frac{d\sigma_{\Upsilon(2S)}}{dy(p_{\mathrm{T}})} \times \mathcal{B}(\Upsilon(2S) \to \mu^+\mu^-)}{\frac{d\sigma_{\Upsilon(1S)}}{dy(p_{\mathrm{T}})} \times \mathcal{B}(\Upsilon(1S) \to \mu^+\mu^-)}, \qquad (3)$$

$$R_{3S/1S} \equiv \frac{\frac{d\sigma_{\Upsilon(3S)}}{dy(p_{\mathrm{T}})} \times \mathcal{B}(\Upsilon(3S) \to \mu^+\mu^-)}{\frac{d\sigma_{\Upsilon(1S)}}{dy(p_{\mathrm{T}})} \times \mathcal{B}(\Upsilon(1S) \to \mu^+\mu^-)}, \qquad (4)$$

and the results are shown in Fig. 6. The ratios increase slightly with p_{T} but show no obvious dependence on y.
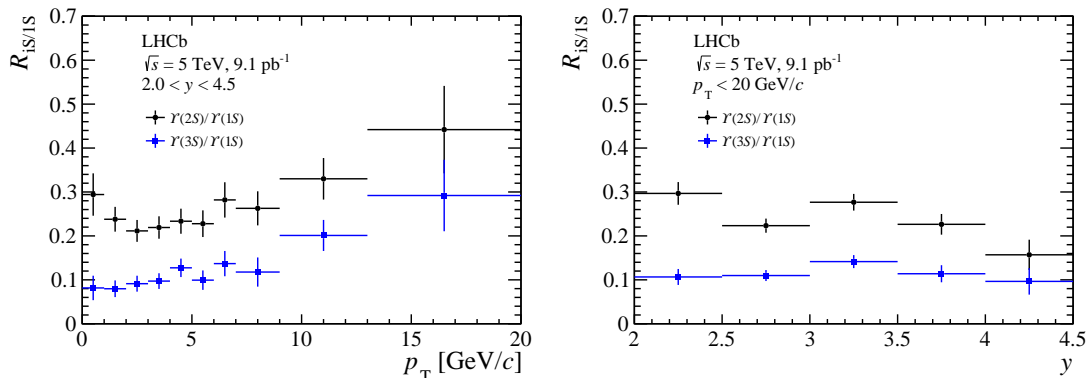
Figure 6: Ratios of the $\Upsilon(2S)$ or $\Upsilon(3S)$ production cross-section over that of the $\Upsilon(1S)$ state, (left) as a function of p_{T} for $2.0 < y < 4.5$ and (right) as a function of y for $p_{\mathrm{T}} < 20\,\mathrm{GeV}/c$. Statistical and systematic uncertainties are added in quadrature.

In the evaluation of the cross-section ratios, the statistical and systematic uncertainties due to the limited simulation sample sizes are assumed to be uncorrelated between the two Υ states and, hence, cancel in the ratios. The systematic uncertainties due to the invariant mass fit model, and those originating from the trigger as well as tracking efficiencies are assumed to be fully correlated between cross-sections of two Υ states.

Using the Υ cross-sections measured by LHCb at $\sqrt{s} = 13\,\mathrm{TeV}$ [20], ratios of cross-sections at $\sqrt{s} = 13\,\mathrm{TeV}$ and $\sqrt{s} = 5\,\mathrm{TeV}$ are determined. The results as a function of p_{T} and those as a function of y are shown in Fig. 7 and are summarized in Tables 6 and 7 in Appendix A , from which it is seen that the ratio increases from about 2 at low p_{T} to about 4 at high p_{T}, but is almost independent of y.

For the cross-section ratios between measurements at different $\sqrt{s}$, the systematic uncertainties due to the invariant mass fit model and final-state radiation are considered to be fully correlated. The systematic uncertainties originating from uncertainties of trigger, muon identification, tracking efficiencies and luminosity are assumed to be partially correlated.
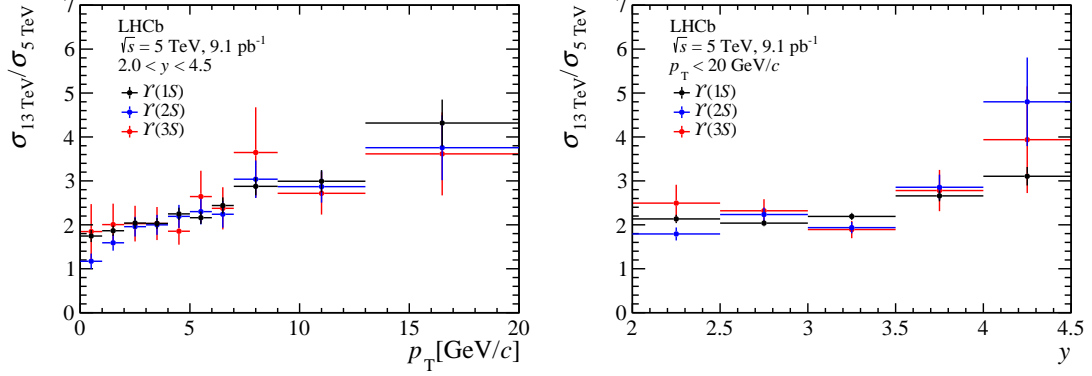
Figure 7: Ratios of Υ production cross-sections measured at $\sqrt{s} = 13\,\mathrm{TeV}$ over those measured at $\sqrt{s} = 5\,\mathrm{TeV}$ (left) as a function of p_T for $2.0 < y < 4.5$ and (right) as a function of y for $p_\mathrm{T} < 20\,\mathrm{GeV}/c$. The statistical and systematic uncertainties are added in quadrature.

5.3 Update of the $\Upsilon(1S)$ nuclear modification factor

To quantify nuclear effects for particle production in heavy-ion collisions, the nuclear modification factor

$$R_{p\mathrm{Pb}} \equiv \frac{\sigma_{p\mathrm{Pb}}(\sqrt{s_{\mathrm{NN}}})}{A \times \sigma_{pp}(\sqrt{s_{\mathrm{NN}}})} \tag{5}$$

is determined, where $A = 208$ is the mass number for Pb, and $\sigma_{p\mathrm{Pb}}$ and σ_{pp} are the cross-sections for proton-lead ($p\mathrm{Pb}$) and pp collisions at the same centre-of-mass energy per nucleon pair. Using a previous measurement of $R_{p\mathrm{Pb}}$ for $\Upsilon(1S)$ in $p\mathrm{Pb}$ collisions at $\sqrt{s_{\mathrm{NN}}} = 5\,\mathrm{TeV}$ [17], the $\Upsilon(1S)$ production cross-section in pp collisions at $\sqrt{s} = 5\,\mathrm{TeV}$ is obtained by an interpolation of LHCb measurements at $\sqrt{s} = 2.76, 7$ and $8\,\mathrm{TeV}$ [18, 48, 49], as

$$\sigma(\Upsilon(1S)) \times \mathcal{B}(\Upsilon(1S) \to \mu^+\mu^-) = 1.12 \pm 0.11\,\mathrm{nb},$$

in the range $p_\mathrm{T} < 15\,\mathrm{GeV}/c, 2.5 < y < 4.0$.

The measurement of the $\Upsilon(1S)$ cross-section times the $\Upsilon(1S) \to \mu^+\mu^-$ branching fraction in the same kinematic range from this analysis is given by

$$\sigma(\Upsilon(1S)) \times \mathcal{B}(\Upsilon(1S) \to \mu^+\mu^-) = 1.34 \pm 0.02 \pm 0.05\,\mathrm{nb},$$

where the first uncertainty is statistical and the second systematic. While the two results are consistent, the direct measurement has an uncertainty that is a factor of two smaller. The nuclear modification factor $R_{p\mathrm{Pb}}$ is updated based on the direct measurement and the results are

$$R_{p\mathrm{Pb}} = \begin{cases} 1.02 \pm 0.19 \pm 0.10 & (-4.0 < y < -2.5), \\ 0.76 \pm 0.08 \pm 0.05 & (2.5 < y < 4.0), \end{cases} \tag{6}$$

where the positive (negative) rapidity is for particles produced in the p (Pb) beam direction. Figure 8 compares the updated result with theoretical calculations considering the EPS09 nuclear parton distribution function [50, 51] or parton energy loss [52], quoted in Ref. [17], and good agreements are found between data and these calculations.
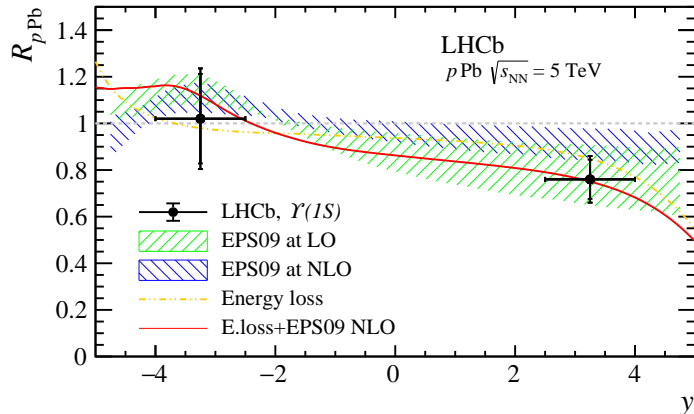
Figure 8: Nuclear modification factor $R_{p\text{Pb}}$ as a function of y for the $\Upsilon(1S)$ state, together with the theoretical predictions mentioned in the text. The inner error bars show the statistical uncertainties, while the outer ones show the statistical and systematic uncertainties added in quadrature.

6 Conclusion

The Υ production cross-sections in proton-proton collisions at a centre-of-mass energy of $\sqrt{s} = 5\,\text{TeV}$ are studied using a data sample with an integrated luminosity of $9.13 \pm 0.18\,\text{pb}^{-1}$, collected by the LHCb detector. The double-differential cross-sections, as function of the transverse momentum p_T and the rapidity y of the Υ mesons, are determined in the range $p_\text{T} < 20\,\text{GeV}/c$ and $2 < y < 4.5$ for the $\Upsilon(1S)$, $\Upsilon(2S)$ and $\Upsilon(3S)$ states. The $\Upsilon(1S)$ cross-section as a function of p_T is well described by the NRQCD calculation for $p_\text{T} > 5\,\text{GeV}/c$ with appropriate long distance matrix elements. The ratios of cross-sections of $\Upsilon(2S)$ and $\Upsilon(3S)$ mesons with respect to $\Upsilon(1S)$ mesons are given in bins of p_T or y. The ratios of cross-sections measured at different pp collision energies are also determined. The nuclear modification factor $R_{p\text{Pb}}$ for $\Upsilon(1S)$ in proton-lead collisions at $\sqrt{s_{\text{NN}}} = 5\,\text{TeV}$ is updated using the $\Upsilon(1S)$ production in pp data measured in this analysis. This result is consistent with the previous result, while improving the precision by a factor of two.

Acknowledgements

Appendices

A   Tabulated results

In the following, Tables 1, 2 and 3 present the double-differential cross-sections times the $\Upsilon \to \mu^+\mu^-$ branching fraction for $\Upsilon(1S)$, $\Upsilon(2S)$ and $\Upsilon(3S)$ mesons, respectively. Tables 4 and 5 present the cross-sections time the $\Upsilon \to \mu^+\mu^-$ branching fraction as a function of p_T, integrated over y, or vice-versa. Tables 6 and 7 present the ratios of cross-sections at $\sqrt{s} = 13\,\mathrm{TeV}$ and $\sqrt{s} = 5\,\mathrm{TeV}$ as a function of p_T and y, respectively.

Table 1: Differential cross-section times the $\Upsilon \to \mu^+\mu^-$ branching fraction (in unit of pb/(GeV/c)) in bins of (p_{T}, y) for the $\Upsilon(1S)$ meson. The first uncertainties are statistical and the second are systematic.

p_{T} (GeV/c)	$2 < y < 2.5$	$2.5 < y < 3$	$3 < y < 3.5$	$3.5 < y < 4$	$4 < y < 4.5$
$0-1$	$50.6 \pm 8.9 \pm 2.3$	$53.6 \pm 6.6 \pm 2.2$	$53.6 \pm 6.7 \pm 2.3$	$45.7 \pm 5.6 \pm 2.1$	$18.2 \pm 4.1 \pm 1.3$
$1-2$	$139.4 \pm 14.8 \pm 6.4$	$129.1 \pm 10.2 \pm 5.1$	$118.4 \pm 9.4 \pm 4.9$	$78.1 \pm 7.5 \pm 3.8$	$65.5 \pm 7.9 \pm 4.6$
$2-3$	$163.2 \pm 16.4 \pm 7.8$	$173.3 \pm 11.5 \pm 6.9$	$141.5 \pm 10.6 \pm 5.8$	$97.0 \pm 8.8 \pm 4.8$	$53.8 \pm 7.5 \pm 3.9$
$3-4$	$168.2 \pm 16.5 \pm 7.5$	$166.6 \pm 11.7 \pm 6.6$	$148.7 \pm 10.5 \pm 6.2$	$109.3 \pm 9.7 \pm 5.8$	$57.8 \pm 8.0 \pm 4.0$
$4-5$	$150.2 \pm 15.3 \pm 6.5$	$149.5 \pm 10.9 \pm 6.0$	$116.4 \pm 9.4 \pm 4.8$	$73.7 \pm 8.1 \pm 4.1$	$47.5 \pm 7.0 \pm 3.3$
$5-6$	$148.0 \pm 15.0 \pm 6.8$	$118.5 \pm 9.8 \pm 4.7$	$99.9 \pm 8.4 \pm 4.2$	$62.7 \pm 7.7 \pm 3.5$	$38.4 \pm 6.8 \pm 2.8$
$6-7$	$101.6 \pm 12.4 \pm 4.7$	$89.4 \pm 8.2 \pm 3.6$	$70.7 \pm 7.1 \pm 3.0$	$53.9 \pm 6.6 \pm 3.0$	$19.9 \pm 5.9 \pm 1.5$
$7-8$	$61.0 \pm 10.2 \pm 2.8$	$66.1 \pm 7.2 \pm 2.6$	$59.2 \pm 6.0 \pm 2.6$	$24.5 \pm 3.5 \pm 1.4$	$16.0 \pm 3.8 \pm 1.2$
$8-9$	$42.1 \pm 8.0 \pm 1.9$	$49.4 \pm 5.8 \pm 2.0$	$34.3 \pm 4.7 \pm 1.5$		
$9-10$	$43.6 \pm 8.3 \pm 2.1$	$39.2 \pm 5.2 \pm 1.6$	$25.7 \pm 4.0 \pm 1.2$	$12.8 \pm 2.0 \pm 0.8$	$4.4 \pm 1.5 \pm 0.3$
$10-13$	$21.0 \pm 3.2 \pm 1.0$	$22.1 \pm 2.2 \pm 0.9$	$11.4 \pm 1.6 \pm 0.5$		
$13-20$	$5.1 \pm 1.1 \pm 0.3$	$3.92 \pm 0.65 \pm 0.20$	$3.20 \pm 0.57 \pm 0.16$	$1.31 \pm 0.45 \pm 0.09$	$0.27 \pm 0.30 \pm 0.02$

Table 2: Differential cross-section times the $\Upsilon \to \mu^+\mu^-$ branching fraction (in unit of pb/(GeV/c)) in bins of (p_T, y) for the $\Upsilon(2S)$ meson. The first uncertainties are statistical and the second are systematic.

p_T (GeV/c)	$2 < y < 2.5$	$2.5 < y < 3$	$3 < y < 3.5$	$3.5 < y < 4$	$4 < y < 4.5$
$0 - 1$	$23.7 \pm 6.5 \pm 1.1$	$6.8 \pm 3.2 \pm 0.3$	$14.4 \pm 4.0 \pm 0.6$	$15.5 \pm 3.4 \pm 0.7$	$4.9 \pm 2.6 \pm 0.3$
$1 - 2$	$38.6 \pm 8.9 \pm 1.8$	$34.4 \pm 5.8 \pm 1.4$	$22.0 \pm 5.3 \pm 1.0$	$26.2 \pm 4.8 \pm 1.3$	$5.0 \pm 3.2 \pm 0.4$
$2 - 3$	$48.0 \pm 9.6 \pm 2.4$	$33.3 \pm 6.0 \pm 1.4$	$41.0 \pm 6.4 \pm 1.8$	$2.8 \pm 4.1 \pm 0.1$	$7.8 \pm 3.5 \pm 0.6$
$3 - 4$	$54.4 \pm 10.4 \pm 2.5$	$30.9 \pm 6.2 \pm 1.3$	$31.9 \pm 5.9 \pm 1.4$	$18.4 \pm 5.2 \pm 1.0$	$7.1 \pm 3.6 \pm 0.5$
$4 - 5$	$44.3 \pm 9.3 \pm 2.0$	$25.5 \pm 5.7 \pm 1.1$	$26.4 \pm 5.4 \pm 1.2$	$19.5 \pm 5.1 \pm 1.1$	$9.7 \pm 3.8 \pm 0.7$
$5 - 6$	$34.1 \pm 8.3 \pm 1.6$	$23.0 \pm 5.5 \pm 1.0$	$33.0 \pm 5.7 \pm 1.5$	$13.3 \pm 4.4 \pm 0.8$	$3.20 \pm 2.93 \pm 0.24$
$6 - 7$	$22.6 \pm 7.7 \pm 1.1$	$18.1 \pm 4.5 \pm 0.8$	$30.5 \pm 5.3 \pm 1.4$	$14.2 \pm 4.3 \pm 0.8$	$9.2 \pm 3.9 \pm 0.7$
$7 - 8$	$18.4 \pm 7.1 \pm 0.9$	$22.1 \pm 4.7 \pm 0.9$	$14.7 \pm 3.5 \pm 0.7$		
$8 - 9$	$3.95 \pm 4.10 \pm 0.18$	$16.0 \pm 3.7 \pm 0.7$	$11.7 \pm 3.2 \pm 0.5$	$7.9 \pm 2.4 \pm 0.5$	$0.38 \pm 2.90 \pm 0.03$
$9 - 10$	$8.8 \pm 4.7 \pm 0.4$	$12.9 \pm 3.8 \pm 0.5$	$9.4 \pm 2.4 \pm 0.4$		
$10 - 13$	$9.4 \pm 2.6 \pm 0.5$	$6.4 \pm 1.4 \pm 0.3$	$4.40 \pm 0.98 \pm 0.21$	$3.49 \pm 1.08 \pm 0.22$	$1.68 \pm 1.00 \pm 0.12$
$13 - 20$	$3.01 \pm 0.86 \pm 0.16$	$1.44 \pm 0.53 \pm 0.07$	$1.09 \pm 0.37 \pm 0.05$	$0.41 \pm 0.37 \pm 0.03$	$0.16 \pm 0.21 \pm 0.02$

Table 3: Differential cross-section times the $\Upsilon \to \mu^+\mu^-$ branching fraction (in unit of pb/(GeV/c)) in bins of (p_{T}, y) for the $\Upsilon(3S)$ meson. The first uncertainties are statistical and the second are systematic.

p_{T} (GeV/c)	$2 < y < 2.5$	$2.5 < y < 3$	$3 < y < 3.5$	$3.5 < y < 4$	$4 < y < 4.5$
$0 - 1$	$4.31 \pm 3.50 \pm 0.21$	$0.68 \pm 2.34 \pm 0.03$	$5.63 \pm 3.23 \pm 0.26$	$5.74 \pm 2.41 \pm 0.28$	$1.72 \pm 1.66 \pm 0.13$
$1 - 2$	$10.53 \pm 6.6 \pm 0.51$	$10.09 \pm 4.33 \pm 0.44$	$14.68 \pm 4.45 \pm 0.68$	$4.56 \pm 3.01 \pm 0.24$	$2.42 \pm 2.62 \pm 0.17$
$2 - 3$	$21.82 \pm 7.16 \pm 1.10$	$13.92 \pm 4.83 \pm 0.61$	$7.44 \pm 4.66 \pm 0.34$	$7.77 \pm 4.15 \pm 0.43$	$6.43 \pm 3.35 \pm 0.48$
$3 - 4$	$7.33 \pm 6.31 \pm 0.35$	$17.17 \pm 5.19 \pm 0.75$	$21.45 \pm 5.12 \pm 0.99$	$9.15 \pm 4.53 \pm 0.54$	$8.10 \pm 3.86 \pm 0.59$
$4 - 5$	$15.12 \pm 6.33 \pm 0.7$	$21.59 \pm 5.18 \pm 0.95$	$20.60 \pm 4.86 \pm 0.96$	$10.02 \pm 4.44 \pm 0.59$	$1.11 \pm 2.87 \pm 0.08$
$5 - 6$	$6.81 \pm 5.67 \pm 0.33$	$11.17 \pm 4.42 \pm 0.49$	$18.19 \pm 4.91 \pm 0.85$	$9.11 \pm 3.98 \pm 0.54$	$1.14 \pm 3.2 \pm 0.09$
$6 - 7$	$10.28 \pm 5.0 \pm 0.51$	$8.07 \pm 3.65 \pm 0.35$	$11.79 \pm 4.30 \pm 0.55$	$9.5 \pm 3.39 \pm 0.56$	$5.76 \pm 3.22 \pm 0.43$
$7 - 8$	$11.90 \pm 5.60 \pm 0.58$	$6.12 \pm 3.45 \pm 0.27$	$6.87 \pm 2.88 \pm 0.32$	$3.65 \pm 2.19 \pm 0.23$	
$8 - 9$	$0.52 \pm 7.65 \pm 0.03$	$10.79 \pm 3.33 \pm 0.47$	$2.8 \pm 2.19 \pm 0.14$		$0.00 \pm 2.21 \pm 0.00$
$9 - 10$	$12.20 \pm 5.10 \pm 0.61$	$3.28 \pm 2.56 \pm 0.14$	$5.02 \pm 1.96 \pm 0.25$		
$10 - 13$	$4.76 \pm 2.02 \pm 0.24$	$3.18 \pm 1.19 \pm 0.14$	$3.47 \pm 0.91 \pm 0.17$	$2.02 \pm 1.03 \pm 0.13$	$1.43 \pm 1.12 \pm 0.10$
$13 - 20$	$1.24 \pm 0.69 \pm 0.07$	$1.64 \pm 0.48 \pm 0.09$	$0.85 \pm 0.34 \pm 0.04$	$0.07 \pm 0.38 \pm 0.00$	$0.23 \pm 0.32 \pm 0.02$

Table 4: Differential cross-section times the $\Upsilon \to \mu^+\mu^-$ branching fraction (in unit of pb/(GeV/c)) of the $\Upsilon(1S)$, $\Upsilon(2S)$ and $\Upsilon(3S)$ mesons as a function of p_T for y integrated from 2.0 to 4.5.

p_T (GeV/c)	$\Upsilon(1S)$	$\Upsilon(2S)$	$\Upsilon(3S)$
$0-1$	$111 \pm 8 \pm 5$	$32.6 \pm 4.7 \pm 1.5$	$9.0 \pm 3.0 \pm 0.5$
$1-2$	$265 \pm 12 \pm 12$	$63.1 \pm 6.6 \pm 2.9$	$21.1 \pm 5.0 \pm 1.0$
$2-3$	$314 \pm 13 \pm 15$	$66.5 \pm 7.0 \pm 3.1$	$28.7 \pm 5.6 \pm 1.5$
$3-4$	$325 \pm 13 \pm 15$	$71.3 \pm 7.5 \pm 3.3$	$31.6 \pm 5.7 \pm 1.6$
$4-5$	$269 \pm 12 \pm 12$	$62.7 \pm 6.9 \pm 3.0$	$34.2 \pm 5.4 \pm 1.6$
$5-6$	$234 \pm 11 \pm 11$	$53.3 \pm 6.3 \pm 2.5$	$23.2 \pm 5.1 \pm 1.2$
$6-7$	$162 \pm 10 \pm 8$	$44.9 \pm 5.7 \pm 2.2$	$22.7 \pm 4.4 \pm 1.2$
$7-9$	$98 \pm 7 \pm 5$	$25.8 \pm 4.4 \pm 1.2$	$11.6 \pm 4.3 \pm 0.6$
$9-13$	$42.6 \pm 3.4 \pm 2.1$	$14.1 \pm 2.2 \pm 0.7$	$8.6 \pm 2.0 \pm 0.5$
$13-20$	$6.9 \pm 0.8 \pm 0.4$	$3.1 \pm 0.6 \pm 0.2$	$2.0 \pm 0.5 \pm 0.1$

Table 5: Differential cross-section times the $\Upsilon \to \mu^+\mu^-$ branching fraction (in unit of pb) of $\Upsilon(1S)$, $\Upsilon(2S)$ and $\Upsilon(3S)$ mesons as a function y for p_T integrated from 0 to 20 GeV/c.

y	$\Upsilon(1S)$	$\Upsilon(2S)$	$\Upsilon(3S)$
$2.0 < y < 2.5$	$1167 \pm 43 \pm 45$	$346 \pm 27 \pm 14$	$124 \pm 21 \pm 5$
$2.5 < y < 3.0$	$1129 \pm 30 \pm 41$	$252 \pm 17 \pm 10$	$124 \pm 14 \pm 5$
$3.0 < y < 3.5$	$925 \pm 26 \pm 35$	$256 \pm 16 \pm 10$	$131 \pm 13 \pm 5$
$3.5 < y < 4.0$	$630 \pm 24 \pm 26$	$143 \pm 14 \pm 6$	$71.7 \pm 12.0 \pm 3.2$
$4.0 < y < 4.5$	$353 \pm 21 \pm 19$	$55 \pm 12 \pm 3$	$34.0 \pm 10.4 \pm 1.8$

Table 6: Cross-section ratios between $\sqrt{s} = 13$ TeV and 5 TeV of $\Upsilon(1S)$, $\Upsilon(2S)$ and $\Upsilon(3S)$ mesons as a function of p_T for y integrated from 2.0 to 4.5.

p_T (GeV/c)	$\Upsilon(1S)$	$\Upsilon(2S)$	$\Upsilon(3S)$
$0-1$	$1.74 \pm 0.12 \pm 0.07$	$1.17 \pm 0.17 \pm 0.05$	$1.85 \pm 0.62 \pm 0.09$
$1-2$	$1.87 \pm 0.08 \pm 0.08$	$1.59 \pm 0.17 \pm 0.07$	$2.00 \pm 0.47 \pm 0.09$
$2-3$	$2.04 \pm 0.08 \pm 0.09$	$1.96 \pm 0.21 \pm 0.09$	$2.03 \pm 0.39 \pm 0.10$
$3-4$	$2.03 \pm 0.08 \pm 0.09$	$2.00 \pm 0.21 \pm 0.09$	$2.03 \pm 0.36 \pm 0.10$
$4-5$	$2.25 \pm 0.10 \pm 0.10$	$2.19 \pm 0.24 \pm 0.10$	$1.85 \pm 0.29 \pm 0.08$
$5-6$	$2.16 \pm 0.10 \pm 0.10$	$2.30 \pm 0.27 \pm 0.10$	$2.64 \pm 0.57 \pm 0.13$
$6-7$	$2.44 \pm 0.15 \pm 0.11$	$2.24 \pm 0.29 \pm 0.11$	$2.38 \pm 0.46 \pm 0.12$
$7-9$	$2.88 \pm 0.15 \pm 0.14$	$3.04 \pm 0.40 \pm 0.15$	$3.65 \pm 1.01 \pm 0.19$
$9-13$	$2.99 \pm 0.17 \pm 0.19$	$2.87 \pm 0.33 \pm 0.16$	$2.72 \pm 0.45 \pm 0.17$
$13-20$	$4.32 \pm 0.48 \pm 0.24$	$3.76 \pm 0.71 \pm 0.21$	$3.61 \pm 0.93 \pm 0.19$

Table 7: Cross-section ratios between $\sqrt{s} = 13\,\text{TeV}$ and $5\,\text{TeV}$ of $\Upsilon(1S)$, $\Upsilon(2S)$ and $\Upsilon(3S)$ mesons as a function of y for p_T integrated from 0 to 20 GeV/c.

y	$\Upsilon(1S)$	$\Upsilon(2S)$	$\Upsilon(3S)$
$2.0 < y < 2.5$	$2.13 \pm 0.08 \pm 0.05$	$1.79 \pm 0.14 \pm 0.05$	$2.49 \pm 0.41 \pm 0.07$
$2.5 < y < 3.0$	$2.04 \pm 0.05 \pm 0.05$	$2.23 \pm 0.15 \pm 0.05$	$2.32 \pm 0.26 \pm 0.06$
$3.0 < y < 3.5$	$2.19 \pm 0.06 \pm 0.05$	$1.94 \pm 0.12 \pm 0.05$	$1.89 \pm 0.19 \pm 0.05$
$3.5 < y < 4.0$	$2.66 \pm 0.10 \pm 0.07$	$2.86 \pm 0.28 \pm 0.08$	$2.78 \pm 0.46 \pm 0.08$
$4.0 < y < 4.5$	$3.11 \pm 0.18 \pm 0.11$	$4.80 \pm 1.00 \pm 0.16$	$3.94 \pm 1.21 \pm 0.13$

B Dependence of cross-sections on the polarisation

The angular distribution of $\Upsilon \to \mu^+\mu^-$ decays is described by

$$\frac{\mathrm{d}^2 N}{\mathrm{d}\cos\theta\mathrm{d}\phi} \propto 1 + \lambda_\theta \cos^2\theta + \lambda_{\theta\phi}\sin 2\theta\cos\phi + \lambda_\phi \sin^2\theta\cos 2\phi, \qquad (1)$$

where θ and ϕ are the polar and azimuthal angles of the μ^+ momentum in the rest frame of the Υ meson for a given polarisation coordinate system, and λ_θ, $\lambda_{\theta\phi}$ and λ_ϕ are the three polarisation parameters [53]. Zero polarisation implies $\lambda_\theta = \lambda_{\theta\phi} = \lambda_\phi = 0$. The detection efficiency of the Υ mesons is a function of the polarisation, especially of λ_θ.

The $\Upsilon(nS)$ mesons are assumed to be unpolarised in this measurement, which is also the case for the simulated signal samples used to determine the efficiencies. Such an assumption is supported by the measurements of the Υ polarization by LHCb in pp collisions at $\sqrt{s} = 7$ TeV and 8 TeV [38] in the same kinematic range as in this analysis, and by the CMS experiment [54] for $\sqrt{s} = 8$ TeV.

To evaluate the change of results assuming non-zero polarisation, the angular distributions of muons in the Υ rest frame in the simulated signal samples are reweighted, and the total efficiencies are recomputed. The relative changes of the double-differential cross-sections for a polarisation of $\lambda_\theta = 0.1$ [38] in the helicity frame compared to zero polarisation in each (p_T,y) interval are given in Tables 8, 9 and 10 for $\Upsilon(1S)$, $\Upsilon(2S)$ and $\Upsilon(3S)$ mesons, respectively. In addition, the relative changes of the double-differential cross-sections for a polarisation of $\lambda_\theta = +1\,(-1)$ are also evaluated, and are shown in Tables 11(14), 12(15) and 13(16) for $\Upsilon(1S)$, $\Upsilon(2S)$ and $\Upsilon(3S)$ mesons, respectively. The helicity frame uses the Υ momentum in the laboratory frame as the spin quantization axis.

Table 8: Relative changes of double-differential cross-sections of $\Upsilon(1S)$ (in %), for a polarisation of $\lambda_\theta = 0.1$ rather than zero, in (p_T,y) intervals.

p_T (GeV/c)	$2 < y < 2.5$	$2.5 < y < 3$	$3 < y < 3.5$	$3.5 < y < 4$	$4 < y < 4.5$
$0 - 1$	2.87 ± 0.37	1.83 ± 0.13	1.01 ± 0.07	1.26 ± 0.13	2.06 ± 0.38
$1 - 2$	2.75 ± 0.21	1.83 ± 0.08	1.06 ± 0.05	1.15 ± 0.08	1.93 ± 0.23
$2 - 3$	2.72 ± 0.18	1.78 ± 0.07	1.10 ± 0.05	1.03 ± 0.08	1.62 ± 0.20
$3 - 4$	2.60 ± 0.17	1.75 ± 0.07	1.03 ± 0.05	0.84 ± 0.08	1.16 ± 0.20
$4 - 5$	2.45 ± 0.17	1.68 ± 0.07	0.94 ± 0.06	0.66 ± 0.10	0.78 ± 0.22
$5 - 6$	2.30 ± 0.19	1.63 ± 0.08	0.78 ± 0.07	0.41 ± 0.11	0.39 ± 0.25
$6 - 7$	2.16 ± 0.21	1.40 ± 0.09	0.61 ± 0.08	0.19 ± 0.14	0.16 ± 0.30
$7 - 8$	2.02 ± 0.23	1.34 ± 0.10	0.47 ± 0.10	-0.05 ± 0.12	-0.24 ± 0.27
$8 - 9$	1.84 ± 0.25	1.25 ± 0.12	0.40 ± 0.11		
$9 - 10$	1.75 ± 0.28	1.14 ± 0.13	0.34 ± 0.14	-0.17 ± 0.14	-0.60 ± 0.32
$10 - 13$	1.48 ± 0.19	1.07 ± 0.09	0.28 ± 0.11		
$13 - 20$	1.34 ± 0.22	0.85 ± 0.11	0.28 ± 0.13	-0.12 ± 0.23	-0.56 ± 0.59

Table 9: Relative changes of cross-sections of $\Upsilon(2S)$ (in %), for a polarisation of $\lambda_\theta = 0.1$ rather than zero, in (p_T,y) intervals.

p_T (GeV/c)	$2 < y < 2.5$	$2.5 < y < 3$	$3 < y < 3.5$	$3.5 < y < 4$	$4 < y < 4.5$
$0-1$	2.83 ± 0.33	1.88 ± 0.14	1.03 ± 0.09	1.29 ± 0.15	2.18 ± 0.40
$1-2$	2.78 ± 0.20	1.83 ± 0.08	1.06 ± 0.05	1.19 ± 0.09	1.96 ± 0.24
$2-3$	2.73 ± 0.17	1.78 ± 0.07	1.06 ± 0.05	1.05 ± 0.08	1.67 ± 0.21
$3-4$	2.61 ± 0.16	1.74 ± 0.07	1.02 ± 0.05	0.89 ± 0.08	1.23 ± 0.20
$4-5$	2.46 ± 0.17	1.68 ± 0.07	0.94 ± 0.06	0.67 ± 0.10	0.84 ± 0.22
$5-6$	2.33 ± 0.18	1.64 ± 0.08	0.83 ± 0.07	0.48 ± 0.11	0.51 ± 0.26
$6-7$	2.18 ± 0.20	1.46 ± 0.08	0.63 ± 0.07	0.24 ± 0.14	0.21 ± 0.30
$7-8$	2.08 ± 0.23	1.41 ± 0.10	0.50 ± 0.09	0.02 ± 0.12	-0.17 ± 0.29
$8-9$	1.88 ± 0.25	1.23 ± 0.10	0.49 ± 0.10		
$9-10$	1.84 ± 0.29	1.16 ± 0.12	0.31 ± 0.12	-0.18 ± 0.15	-0.45 ± 0.33
$10-13$	1.59 ± 0.20	1.11 ± 0.08	0.27 ± 0.10		
$13-20$	1.34 ± 0.20	0.89 ± 0.08	0.28 ± 0.11	-0.15 ± 0.22	-0.57 ± 0.65

Table 10: Relative changes of cross-sections of $\Upsilon(3S)$ (in %), for a polarisation of $\lambda_\theta = 0.1$ rather than zero, in (p_T,y) intervals

p_T (GeV/c)	$2 < y < 2.5$	$2.5 < y < 3$	$3 < y < 3.5$	$3.5 < y < 4$	$4 < y < 4.5$
$0-1$	2.81 ± 0.32	1.87 ± 0.13	1.04 ± 0.08	1.22 ± 0.14	2.27 ± 0.44
$1-2$	2.77 ± 0.20	1.84 ± 0.08	1.06 ± 0.05	1.20 ± 0.09	1.97 ± 0.24
$2-3$	2.72 ± 0.17	1.81 ± 0.07	1.07 ± 0.05	1.09 ± 0.08	1.64 ± 0.21
$3-4$	2.62 ± 0.16	1.77 ± 0.07	1.02 ± 0.05	0.91 ± 0.08	1.28 ± 0.20
$4-5$	2.54 ± 0.18	1.70 ± 0.07	0.95 ± 0.06	0.72 ± 0.10	0.91 ± 0.22
$5-6$	2.33 ± 0.18	1.65 ± 0.08	0.84 ± 0.07	0.51 ± 0.11	0.56 ± 0.27
$6-7$	2.21 ± 0.21	1.51 ± 0.09	0.69 ± 0.08	0.29 ± 0.14	0.29 ± 0.31
$7-8$	2.11 ± 0.24	1.43 ± 0.10	0.53 ± 0.09	0.09 ± 0.12	-0.06 ± 0.28
$8-9$	1.94 ± 0.26	1.23 ± 0.10	0.44 ± 0.10		
$9-10$	1.74 ± 0.28	1.22 ± 0.11	0.42 ± 0.10	-0.11 ± 0.14	-0.52 ± 0.33
$10-13$	1.60 ± 0.19	1.05 ± 0.07	0.31 ± 0.08		
$13-20$	1.42 ± 0.21	0.87 ± 0.07	0.34 ± 0.08	-0.11 ± 0.18	-0.55 ± 0.62

Table 11: Relative changes of cross-sections of $\Upsilon(1S)$ (in %), for a polarisation of $\lambda_\theta = 1$ rather than zero, in (p_T,y) intervals

p_T (GeV/c)	$2 < y < 2.5$	$2.5 < y < 3$	$3 < y < 3.5$	$3.5 < y < 4$	$4 < y < 4.5$
$0-1$	27.5 ± 1.5	16.2 ± 0.5	8.4 ± 0.3	10.7 ± 0.5	18.8 ± 1.4
$1-2$	26.3 ± 0.8	16.2 ± 0.3	8.8 ± 0.2	9.7 ± 0.3	17.2 ± 0.9
$2-3$	25.8 ± 0.7	15.7 ± 0.3	9.2 ± 0.2	8.6 ± 0.3	14.2 ± 0.7
$3-4$	24.4 ± 0.7	15.4 ± 0.3	8.6 ± 0.2	6.9 ± 0.3	9.8 ± 0.6
$4-5$	22.7 ± 0.7	14.7 ± 0.3	7.8 ± 0.2	5.3 ± 0.3	6.4 ± 0.7
$5-6$	21.1 ± 0.7	14.2 ± 0.3	6.4 ± 0.2	3.3 ± 0.3	3.1 ± 0.7
$6-7$	19.5 ± 0.8	12.1 ± 0.3	4.9 ± 0.3	1.5 ± 0.4	1.3 ± 0.9
$7-8$	18.0 ± 0.8	11.4 ± 0.4	3.8 ± 0.3	-0.4 ± 0.3	-1.8 ± 0.7
$8-9$	16.3 ± 0.9	10.6 ± 0.4	3.2 ± 0.4		
$9-10$	15.4 ± 1.0	9.6 ± 0.5	2.7 ± 0.4	-1.3 ± 0.4	-4.5 ± 0.8
$10-13$	12.8 ± 0.7	8.9 ± 0.3	2.2 ± 0.3		
$13-20$	11.4 ± 0.8	7.0 ± 0.4	2.2 ± 0.4	-0.9 ± 0.6	-4.2 ± 1.5

Table 12: Relative changes of cross-sections of $\Upsilon(2S)$ (in %), for a polarisation of $\lambda_\theta = 1$ rather than zero, in (p_T,y) intervals.

p_T (GeV/c)	$2 < y < 2.5$	$2.5 < y < 3$	$3 < y < 3.5$	$3.5 < y < 4$	$4 < y < 4.5$
$0-1$	27.2 ± 1.3	16.7 ± 0.5	8.5 ± 0.3	11.0 ± 0.5	19.8 ± 1.5
$1-2$	26.6 ± 0.8	16.2 ± 0.3	8.8 ± 0.2	10.0 ± 0.3	17.6 ± 0.9
$2-3$	25.9 ± 0.7	15.7 ± 0.3	8.9 ± 0.2	8.8 ± 0.3	14.6 ± 0.7
$3-4$	24.5 ± 0.6	15.3 ± 0.3	8.5 ± 0.2	7.3 ± 0.3	10.4 ± 0.7
$4-5$	22.9 ± 0.6	14.7 ± 0.3	7.8 ± 0.2	5.5 ± 0.3	6.9 ± 0.7
$5-6$	21.5 ± 0.7	14.3 ± 0.3	6.8 ± 0.2	3.8 ± 0.3	4.1 ± 0.8
$6-7$	19.8 ± 0.8	12.5 ± 0.3	5.1 ± 0.3	1.9 ± 0.4	1.7 ± 0.9
$7-8$	18.6 ± 0.9	12.1 ± 0.4	4.0 ± 0.3	0.2 ± 0.4	-1.3 ± 0.8
$8-9$	16.7 ± 0.9	10.4 ± 0.4	3.9 ± 0.3		
$9-10$	16.1 ± 1.1	9.8 ± 0.5	2.5 ± 0.4	-1.4 ± 0.4	-3.4 ± 0.9
$10-13$	13.7 ± 0.7	9.2 ± 0.3	2.1 ± 0.3		
$13-20$	11.5 ± 0.7	7.3 ± 0.3	2.2 ± 0.4	-1.2 ± 0.6	-4.3 ± 1.6

Table 13: Relative changes of cross-sections of $\Upsilon(3S)$ (in %), for a polarisation of $\lambda_\theta = 1$ rather than zero, in (p_T,y) intervals.

p_T (GeV/c)	$2 < y < 2.5$	$2.5 < y < 3$	$3 < y < 3.5$	$3.5 < y < 4$	$4 < y < 4.5$
$0 - 1$	27.0 ± 1.3	16.6 ± 0.5	8.7 ± 0.3	10.3 ± 0.5	20.6 ± 1.6
$1 - 2$	26.5 ± 0.8	16.3 ± 0.3	8.9 ± 0.2	10.1 ± 0.3	17.6 ± 0.9
$2 - 3$	25.9 ± 0.7	15.9 ± 0.3	8.9 ± 0.2	9.2 ± 0.3	14.4 ± 0.7
$3 - 4$	24.6 ± 0.6	15.5 ± 0.3	8.5 ± 0.2	7.5 ± 0.3	10.9 ± 0.7
$4 - 5$	23.6 ± 0.7	14.9 ± 0.3	7.9 ± 0.2	5.9 ± 0.3	7.5 ± 0.7
$5 - 6$	21.5 ± 0.7	14.4 ± 0.3	6.9 ± 0.2	4.1 ± 0.4	4.5 ± 0.8
$6 - 7$	20.2 ± 0.8	13.0 ± 0.4	5.6 ± 0.3	2.3 ± 0.4	2.3 ± 0.9
$7 - 8$	18.9 ± 0.9	12.3 ± 0.4	4.3 ± 0.3	0.7 ± 0.4	-0.5 ± 0.8
$8 - 9$	17.3 ± 1.0	10.4 ± 0.4	3.5 ± 0.3		
$9 - 10$	15.3 ± 1.0	10.3 ± 0.5	3.4 ± 0.4	-0.8 ± 0.4	-3.8 ± 0.9
$10 - 13$	14.0 ± 0.7	8.8 ± 0.3	2.4 ± 0.3		
$13 - 20$	12.1 ± 0.7	7.2 ± 0.3	2.7 ± 0.3	-0.8 ± 0.5	-4.2 ± 1.6

Table 14: Relative changes of cross-sections of $\Upsilon(1S)$ (in %), for a polarisation of $\lambda_\theta = -1$ rather than zero, in (p_T,y) intervals.

p_T (GeV/c)	$2 < y < 2.5$	$2.5 < y < 3$	$3 < y < 3.5$	$3.5 < y < 4$	$4 < y < 4.5$
$0 - 1$	-30.2 ± 0.7	-21.7 ± 0.1	-13.4 ± 0.2	-16.1 ± 0.1	-23.6 ± 0.7
$1 - 2$	-29.1 ± 0.4	-21.8 ± 0.1	-13.9 ± 0.2	-14.9 ± 0.1	-22.6 ± 0.5
$2 - 3$	-29.1 ± 0.3	-21.4 ± 0.1	-14.4 ± 0.1	-13.6 ± 0.1	-19.8 ± 0.5
$3 - 4$	-28.3 ± 0.3	-21.0 ± 0.1	-13.7 ± 0.1	-11.4 ± 0.2	-15.1 ± 0.5
$4 - 5$	-27.0 ± 0.3	-20.4 ± 0.1	-12.7 ± 0.1	-9.3 ± 0.3	-10.6 ± 0.7
$5 - 6$	-25.9 ± 0.4	-20.1 ± 0.1	-10.7 ± 0.2	-6.0 ± 0.4	-5.6 ± 0.9
$6 - 7$	-24.8 ± 0.5	-17.5 ± 0.1	-8.5 ± 0.2	-2.9 ± 0.5	-2.4 ± 1.2
$7 - 8$	-23.6 ± 0.5	-16.9 ± 0.1	-6.7 ± 0.3	0.7 ± 0.5	3.9 ± 1.2
$8 - 9$	-21.8 ± 0.6	-16.1 ± 0.2	-5.8 ± 0.3		
$9 - 10$	-21.1 ± 0.7	-14.7 ± 0.2	-5.0 ± 0.4	2.7 ± 0.6	10.5 ± 1.5
$10 - 13$	-18.3 ± 0.5	-14.1 ± 0.1	-4.2 ± 0.3		
$13 - 20$	-17.0 ± 0.6	-11.6 ± 0.2	-4.2 ± 0.4	1.9 ± 0.9	9.5 ± 2.8

Table 15: Relative changes of cross-sections of $\Upsilon(2S)$ (in %), for a polarisation of $\lambda_\theta = -1$ rather than zero, in (p_T,y) intervals.

p_T (GeV/c)	$2 < y < 2.5$	$2.5 < y < 3$	$3 < y < 3.5$	$3.5 < y < 4$	$4 < y < 4.5$
$0-1$	-29.7 ± 0.7	-22.3 ± 0.2	-13.6 ± 0.1	-16.6 ± 0.3	-24.8 ± 0.8
$1-2$	-29.5 ± 0.4	-21.8 ± 0.1	-13.9 ± 0.1	-15.4 ± 0.2	-22.9 ± 0.5
$2-3$	-29.2 ± 0.3	-21.3 ± 0.1	-14.0 ± 0.1	-13.9 ± 0.2	-20.4 ± 0.5
$3-4$	-28.2 ± 0.3	-21.0 ± 0.1	-13.5 ± 0.1	-12.0 ± 0.2	-15.8 ± 0.5
$4-5$	-27.1 ± 0.3	-20.3 ± 0.1	-12.7 ± 0.1	-9.4 ± 0.3	-11.4 ± 0.7
$5-6$	-26.1 ± 0.4	-20.2 ± 0.1	-11.3 ± 0.1	-6.8 ± 0.3	-7.3 ± 0.9
$6-7$	-24.9 ± 0.4	-18.1 ± 0.1	-8.8 ± 0.2	-3.5 ± 0.5	-3.2 ± 1.1
$7-8$	-24.2 ± 0.5	-17.8 ± 0.1	-7.1 ± 0.2	-0.3 ± 0.5	2.7 ± 1.3
$8-9$	-22.2 ± 0.5	-15.9 ± 0.2	-7.1 ± 0.2		
$9-10$	-22.2 ± 0.6	-15.0 ± 0.2	-4.5 ± 0.4	2.9 ± 0.6	7.8 ± 1.6
$10-13$	-19.6 ± 0.4	-14.6 ± 0.2	-4.1 ± 0.3		
$13-20$	-16.9 ± 0.4	-12.1 ± 0.3	-4.2 ± 0.3	2.4 ± 0.9	9.8 ± 3.2

Table 16: Relative changes of cross-sections of $\Upsilon(3S)$ (in %), for a polarisation of $\lambda_\theta = -1$ rather than zero, in (p_T,y) intervals.

p_T (GeV/c)	$2 < y < 2.5$	$2.5 < y < 3$	$3 < y < 3.5$	$3.5 < y < 4$	$4 < y < 4.5$
$0-1$	-29.7 ± 0.6	-22.2 ± 0.2	-13.7 ± 0.1	-15.6 ± 0.3	-25.8 ± 0.9
$1-2$	-29.3 ± 0.4	-22.0 ± 0.1	-14.0 ± 0.1	-15.6 ± 0.2	-22.9 ± 0.5
$2-3$	-29.1 ± 0.3	-21.7 ± 0.1	-14.1 ± 0.1	-14.4 ± 0.2	-19.9 ± 0.5
$3-4$	-28.3 ± 0.3	-21.2 ± 0.1	-13.6 ± 0.1	-12.3 ± 0.2	-16.5 ± 0.5
$4-5$	-27.9 ± 0.4	-20.6 ± 0.1	-12.8 ± 0.1	-10.0 ± 0.3	-12.2 ± 0.7
$5-6$	-26.1 ± 0.4	-20.1 ± 0.1	-11.5 ± 0.1	-7.3 ± 0.4	-8.0 ± 0.9
$6-7$	-25.1 ± 0.4	-18.8 ± 0.1	-9.6 ± 0.2	-4.3 ± 0.5	-4.4 ± 1.1
$7-8$	-24.4 ± 0.5	-18.0 ± 0.1	-7.6 ± 0.2	-1.4 ± 0.5	1.0 ± 1.2
$8-9$	-22.8 ± 0.5	-15.8 ± 0.2	-6.4 ± 0.2		
$9-10$	-20.9 ± 0.6	-15.7 ± 0.3	-6.1 ± 0.2	1.7 ± 0.6	8.8 ± 1.6
$10-13$	-19.5 ± 0.4	-13.8 ± 0.2	-4.6 ± 0.2		
$13-20$	-18.0 ± 0.4	-11.8 ± 0.3	-5.0 ± 0.2	1.7 ± 0.7	9.3 ± 2.9

References

[1] C. E. Carlson and R. Suaya, *Hadronic production of J/ψ mesons*, Phys. Rev. **D14** (1976) 3115.

[2] A. Donnachie and P. V. Landshoff, *Production of lepton pairs, J/ψ and charm with hadron beams*, Nucl. Phys. **B112** (1976) 233.

[3] S. D. Ellis, M. B. Einhorn, and C. Quigg, *Comment on hadronic production of psions*, Phys. Rev. Lett. **36** (1976) 1263.

[4] H. Fritzsch, *Producing heavy quark flavors in hadronic collisions: A test of quantum chromodynamics*, Phys. Lett. **B67** (1977) 217.

[5] M. Glück, J. F. Owens, and E. Reya, *Gluon contribution to hadronic J/ψ production*, AIP Conf. Proc. **43** (1978) 467.

[6] C.-H. Chang, *Hadronic production of J/ψ associated with a gluon*, Nucl. Phys. **B172** (1980) 425.

[7] R. Baier and R. Ruckl, *Hadronic production of J/ψ and Υ: Transverse momentum distributions*, Phys. Lett. **B102** (1981) 364.

[8] F. Halzen, *CVC for gluons and hadroproduction of quark flavors*, Phys. Lett. **B69** (1977) 105.

[9] M. Gluck, J. F. Owens, and E. Reya, *Gluon contribution to hadronic J/ψ production*, Phys. Rev. **D17** (1978) 2324.

[10] J. R. Wu, *Mechanisms for (p, p') reactions in the continuum*, Phys. Lett. **B91** (1980) 169.

[11] G. T. Bodwin, E. Braaten, and G. P. Lepage, *Rigorous QCD analysis of inclusive annihilation and production of heavy quarkonium*, Phys. Rev. **D51** (1995) 1125, Erratum ibid. **55** (1997) 5853, `arXiv:hep-ph/9407339`.

[12] P. L. Cho and A. K. Leibovich, *Color octet quarkonia production*, Phys. Rev. **D53** (1996) 150, `arXiv:hep-ph/9505329`.

[13] P. L. Cho and A. K. Leibovich, *Color octet quarkonia production.2*, Phys. Rev. **D53** (1996) 6203, `arXiv:hep-ph/9511315`.

[14] A.-P. Chen, Y.-Q. Ma, and H. Zhang, *A Short Theoretical Review of Charmonium Production*, Adv. High Energy Phys. **2022** (2022) 7475923, `arXiv:2109.04028`.

[15] N. Brambilla *et al.*, *Heavy quarkonium: progress, puzzles, and opportunities*, Eur. Phys. J. **C71** (2011) 1534, `arXiv:1010.5827`.

[16] E. Chapon *et al.*, *Prospects for quarkonium studies at the high-luminosity LHC*, Prog. Part. Nucl. Phys. **122** (2022) 103906, `arXiv:2012.14161`.

[17] LHCb collaboration, R. Aaij *et al.*, *Study of Υ production and cold nuclear matter effects in pPb collisions at $\sqrt{s_{NN}} = 5$ TeV*, JHEP **07** (2014) 094, `arXiv:1405.5152`.

[18] LHCb collaboration, R. Aaij *et al.*, *Measurement of Υ production in pp collisions at $\sqrt{s} = 2.76\,TeV$*, Eur. Phys. J. **C74** (2014) 2835, arXiv:1402.2539.

[19] LHCb collaboration, R. Aaij *et al.*, *Forward production of Υ mesons in pp collisions at $\sqrt{s} = 7$ and 8 TeV*, JHEP **11** (2015) 103, arXiv:1509.02372.

[20] LHCb collaboration, R. Aaij *et al.*, *Measurement of Υ production cross-section in pp collisions at $\sqrt{s} = 13\,TeV$*, JHEP **07** (2018) 134, arXiv:1804.09214.

[21] LHCb collaboration, R. Aaij *et al.*, *Precision luminosity measurements at LHCb*, JINST **9** (2014) P12005, arXiv:1410.0149.

[22] LHCb collaboration, A. A. Alves Jr. *et al.*, *The LHCb detector at the LHC*, JINST **3** (2008) S08005.

[23] LHCb collaboration, R. Aaij *et al.*, *LHCb detector performance*, Int. J. Mod. Phys. **A30** (2015) 1530022, arXiv:1412.6352.

[24] R. Aaij *et al.*, *Performance of the LHCb Vertex Locator*, JINST **9** (2014) P09007, arXiv:1405.7808.

[25] P. d'Argent *et al.*, *Improved performance of the LHCb Outer Tracker in LHC Run 2*, JINST **12** (2017) P11016, arXiv:1708.00819.

[26] A. A. Alves Jr. *et al.*, *Performance of the LHCb muon system*, JINST **8** (2013) P02022, arXiv:1211.1346.

[27] R. Aaij *et al.*, *The LHCb trigger and its performance in 2011*, JINST **8** (2013) P04022, arXiv:1211.3055.

[28] G. Dujany and B. Storaci, *Real-time alignment and calibration of the LHCb Detector in Run II*, J. Phys. Conf. Ser. **664** (2015) 082010.

[29] R. Aaij *et al.*, *Tesla: an application for real-time data analysis in High Energy Physics*, Comput. Phys. Commun. **208** (2016) 35, arXiv:1604.05596.

[30] T. Sjöstrand, S. Mrenna, and P. Skands, *A brief introduction to PYTHIA 8.1*, Comput. Phys. Commun. **178** (2008) 852, arXiv:0710.3820; T. Sjöstrand, S. Mrenna, and P. Skands, *PYTHIA 6.4 physics and manual*, JHEP **05** (2006) 026, arXiv:hep-ph/0603175.

[31] I. Belyaev *et al.*, *Handling of the generation of primary events in Gauss, the LHCb simulation framework*, J. Phys. Conf. Ser. **331** (2011) 032047.

[32] D. J. Lange, *The EvtGen particle decay simulation package*, Nucl. Instrum. Meth. **A462** (2001) 152.

[33] N. Davidson, T. Przedzinski, and Z. Was, *PHOTOS interface in C++: Technical and physics documentation*, Comp. Phys. Comm. **199** (2016) 86, arXiv:1011.0937.

[34] Geant4 collaboration, J. Allison *et al.*, *Geant4 developments and applications*, IEEE Trans. Nucl. Sci. **53** (2006) 270; Geant4 collaboration, S. Agostinelli *et al.*, *Geant4: A simulation toolkit*, Nucl. Instrum. Meth. **A506** (2003) 250.

[35] M. Clemencic *et al.*, *The LHCb simulation application, Gauss: Design, evolution and experience*, J. Phys. Conf. Ser. **331** (2011) 032023.

[36] T. Skwarnicki, *A study of the radiative cascade transitions between the Upsilon-prime and Upsilon resonances*, PhD thesis, Institute of Nuclear Physics, Krakow, 1986, DESY-F31-86-02.

[37] Particle Data Group, R. L. Workman and Others, *Review of Particle Physics*, PTEP **2022** (2022) 083C01.

[38] LHCb collaboration, R. Aaij *et al.*, *Measurement of the $\Upsilon(nS)$ polarizations in pp collisions at $\sqrt{s} = 7$ and 8 TeV*, JHEP **12** (2017) 110, `arXiv:1709.01301`.

[39] LHCb collaboration, R. Aaij *et al.*, *Measurement of J/ψ production in pp collisions at $\sqrt{s} = 7$ TeV*, Eur. Phys. J. **C71** (2011) 1645, `arXiv:1103.0423`.

[40] F. Archilli *et al.*, *Performance of the muon identification at LHCb*, JINST **8** (2013) P10020, `arXiv:1306.0249`.

[41] R. Aaij *et al.*, *Selection and processing of calibration samples to measure the particle identification performance of the LHCb experiment in Run 2*, Eur. Phys. J. Tech. Instr. **6** (2019) 1, `arXiv:1803.00824`.

[42] LHCb collaboration, R. Aaij *et al.*, *Measurement of J/ψ production cross-sections in pp collisions at $\sqrt{s} = 5$ TeV*, JHEP **11** (2021) 181, `arXiv:2109.00220`.

[43] R. Aaij *et al.*, *Performance of the LHCb trigger and full real-time reconstruction in Run 2 of the LHC*, JINST **14** (2019) P04013, `arXiv:1812.10790`.

[44] LHCb collaboration, R. Aaij *et al.*, *Measurement of the track reconstruction efficiency at LHCb*, JINST **10** (2015) P02007, `arXiv:1408.1251`.

[45] M. Pivk and F. R. Le Diberder, *sPlot: A statistical tool to unfold data distributions*, Nucl. Instrum. Meth. **A555** (2005) 356, `arXiv:physics/0402083`.

[46] Y. Feng, B. Gong, L.-P. Wan, and J.-X. Wang, *An updated study of Υ production and polarization at the Tevatron and LHC*, Chin. Phys. C **39** (2015) 123102, `arXiv:1503.08439`.

[47] H. Han *et al.*, *Υ and $\chi_b(nP)$ production at hadron colliders in nonrelativistic QCD*, Phys. Rev. **D94** (2016) 014028, `arXiv:1410.8537`.

[48] LHCb collaboration, R. Aaij *et al.*, *Production of J/ψ and Υ mesons in pp collisions at $\sqrt{s} = 8$ TeV*, JHEP **06** (2013) 064, `arXiv:1304.6977`.

[49] LHCb collaboration, R. Aaij *et al.*, *Measurement of Υ production in pp collisions at $\sqrt{s} = 7$ TeV*, Eur. Phys. J. **C72** (2012) 2025, `arXiv:1202.6579`.

[50] J. L. Albacete *et al.*, *Predictions for p+Pb collisions at $\sqrt{s_{NN}} = 5$ TeV*, Int. J. Mod. Phys. **E22** (2013) 1330007, `arXiv:1301.3395`.

[51] E. G. Ferreiro *et al.*, *Upsilon production in p(d)A collisions at RHIC and the LHC*, Eur. Phys. J. **C73** (2013) 2427, `arXiv:1110.5047`.

[52] F. Arleo and S. Peigne, *Heavy-quarkonium suppression in p-A collisions from parton energy loss in cold QCD matter*, JHEP **03** (2013) 122, `arXiv:1212.0434`.

[53] P. Faccioli, C. Lourenco, J. Seixas, and H. K. Wohri, *Towards the experimental clarification of quarkonium polarization*, Eur. Phys. J. C **69** (2010) 657, `arXiv:1006.2738`.

[54] CMS collaboration, S. Chatrchyan *et al.*, *Measurement of the $\Upsilon(1S), \Upsilon(2S)$ and $\Upsilon(3S)$ polarizations in pp collisions at $\sqrt{s} = 7$ TeV*, Phys. Rev. Lett. **110** (2013) 081802, `arXiv:1209.2922`.

LHCb collaboration

R. Aaij[32] , A.S.W. Abdelmotteleb[50] , C. Abellan Beteta[44], F. Abudinén[50] ,

T. Ackernley[54] , B. Adeva[40] , M. Adinolfi[48] , P. Adlarson[77] , H. Afsharnia[9],

C. Agapopoulou[13] , C.A. Aidala[78] , Z. Ajaltouni[9], S. Akar[59] , K. Akiba[32] ,

P. Albicocco[23] , J. Albrecht[15] , F. Alessio[42] , M. Alexander[53] , A. Alfonso Albero[39] ,

Z. Aliouche[56] , P. Alvarez Cartelle[49] , R. Amalric[13] , S. Amato[2] , J.L. Amey[48] ,

Y. Amhis[11,42] , L. An[42] , L. Anderlini[22] , M. Andersson[44] , A. Andreianov[38] ,

M. Andreotti[21] , D. Andreou[62] , D. Ao[6] , F. Archilli[17] , A. Artamonov[38] ,

M. Artuso[62] , E. Aslanides[10] , M. Atzeni[44] , B. Audurier[12] , I.B Bachiller Perea[8] ,

S. Bachmann[17] , M. Bachmayer[43] , J.J. Back[50] , A. Bailly-reyre[13],

P. Baladron Rodriguez[40] , V. Balagura[12] , W. Baldini[21,42] , J. Baptista de Souza Leite[1] ,

M. Barbetti[22,k] , R.J. Barlow[56] , S. Barsuk[11] , W. Barter[52] , M. Bartolini[49] ,

F. Baryshnikov[38] , J.M. Basels[14] , G. Bassi[29,q] , B. Batsukh[4] , A. Battig[15] ,

A. Bay[43] , A. Beck[50] , M. Becker[15] , F. Bedeschi[29] , I.B. Bediaga[1] , A. Beiter[62],

V. Belavin[38], S. Belin[40] , V. Bellee[44] , K. Belous[38] , I. Belov[38] , I. Belyaev[38] ,

G. Benane[10] , G. Bencivenni[23] , E. Ben-Haim[13] , A. Berezhnoy[38] , R. Bernet[44] ,

S. Bernet Andres[76] , D. Berninghoff[17], H.C. Bernstein[62], C. Bertella[56] , A. Bertolin[28] ,

C. Betancourt[44] , F. Betti[42] , Ia. Bezshyiko[44] , S. Bhasin[48] , J. Bhom[35] , L. Bian[68] ,

M.S. Bieker[15] , N.V. Biesuz[21] , P. Billoir[13] , A. Biolchini[32] , M. Birch[55] ,

F.C.R. Bishop[49] , A. Bitadze[56] , A. Bizzeti , M.P. Blago[49] , T. Blake[50] , F. Blanc[43] ,

J.E. Blank[15] , S. Blusk[62] , D. Bobulska[53] , J.A. Boelhauve[15] , O. Boente Garcia[12] ,

T. Boettcher[59] , A. Boldyrev[38] , C.S. Bolognani[74] , R. Bolzonella[21,j] , N. Bondar[38,42] ,

F. Borgato[28] , S. Borghi[56] , M. Borsato[17] , J.T. Borsuk[35] , S.A. Bouchiba[43] ,

T.J.V. Bowcock[54] , A. Boyer[42] , C. Bozzi[21] , M.J. Bradley[55], S. Braun[60] ,

A. Brea Rodriguez[40] , J. Brodzicka[35] , A. Brossa Gonzalo[40] , J. Brown[54] ,

D. Brundu[27] , A. Buonaura[44] , L. Buonincontri[28] , A.T. Burke[56] , C. Burr[42] ,

A. Bursche[66], A. Butkevich[38] , J.S. Butter[32] , J. Buytaert[42] , W. Byczynski[42] ,

S. Cadeddu[27] , H. Cai[68], R. Calabrese[21,j] , L. Calefice[15] , S. Cali[23] , M. Calvi[26,n] ,

M. Calvo Gomez[76] , P. Campana[23] , D.H. Campora Perez[74] ,

A.F. Campoverde Quezada[6] , S. Capelli[26,n] , L. Capriotti[20] , A. Carbone[20,h] ,

R. Cardinale[24,l] , A. Cardini[27] , P. Carniti[26,n] , L. Carus[14], A. Casais Vidal[40] ,

R. Caspary[17] , G. Casse[54] , M. Cattaneo[42] , G. Cavallero[55,42] , V. Cavallini[21,j] ,

S. Celani[43] , J. Cerasoli[10] , D. Cervenkov[57] , A.J. Chadwick[54] , I. Chahrour[78] ,

M.G. Chapman[48], M. Charles[13] , Ph. Charpentier[42] , C.A. Chavez Barajas[54] ,

M. Chefdeville[8] , C. Chen[3] , S. Chen[4] , A. Chernov[35] , S. Chernyshenko[46] ,

V. Chobanova[40] , S. Cholak[43] , M. Chrzaszcz[35] , A. Chubykin[38] , V. Chulikov[38] ,

P. Ciambrone[23] , M.F. Cicala[50] , X. Cid Vidal[40] , G. Ciezarek[42] , P. Cifra[42] ,

G. Ciullo[j,21] , P.E.L. Clarke[52] , M. Clemencic[42] , H.V. Cliff[49] , J. Closier[42] ,

J.L. Cobbledick[56] , V. Coco[42] , J.A.B. Coelho[11] , J. Cogan[10] , E. Cogneras[9] ,

L. Cojocariu[37] , P. Collins[42] , T. Colombo[42] , L. Congedo[19] , A. Contu[27] ,

N. Cooke[47] , I. Corredoira [40] , G. Corti[42] , B. Couturier[42] , D.C. Craik[44] ,

M. Cruz Torres[1,f] , R. Currie[52] , C.L. Da Silva[61] , S. Dadabaev[38] , L. Dai[65] ,

X. Dai[5] , E. Dall'Occo[15] , J. Dalseno[40] , C. D'Ambrosio[42] , J. Daniel[9] ,

A. Danilina[38] , P. d'Argent[19] , J.E. Davies[56] , A. Davis[56] , O. De Aguiar Francisco[56] ,

J. de Boer[42] , K. De Bruyn[73] , S. De Capua[56] , M. De Cian[43] ,

U. De Freitas Carneiro Da Graca[1] , E. De Lucia[23] , J.M. De Miranda[1] , L. De Paula[2] ,

M. De Serio[19,g] , D. De Simone[44] , P. De Simone[23] , F. De Vellis[15] , J.A. de Vries[74] ,

C.T. Dean[61] , F. Debernardis[19,g] , D. Decamp[8] , V. Dedu[10] , L. Del Buono[13] ,

B. Delaney[58] , H.-P. Dembinski[15] , V. Denysenko[44] , O. Deschamps[9] , F. Dettori[27,i] ,

B. Dey[71] , P. Di Nezza[23] , I. Diachkov[38] , S. Didenko[38] , L. Dieste Maronas[40],

S. Ding[62] , V. Dobishuk[46] , A. Dolmatov[38], C. Dong[3] , A.M. Donohoe[18] , F. Dordei[27] ,

A.C. dos Reis[1] , L. Douglas[53], A.G. Downes[8] , P. Duda[75] , M.W. Dudek[35] ,

L. Dufour[42] , V. Duk[72] , P. Durante[42] , M. M. Duras[75] , J.M. Durham[61] ,

D. Dutta[56] , A. Dziurda[35] , A. Dzyuba[38] , S. Easo[51] , U. Egede[63] , V. Egorychev[38] ,

C. Eirea Orro[40], S. Eisenhardt[52] , E. Ejopu[56] , S. Ek-In[43] , L. Eklund[77] ,

J. Ellbracht[15] , S. Ely[55] , A. Ene[37] , E. Epple[59] , S. Escher[14] , J. Eschle[44] ,

S. Esen[44] , T. Evans[56] , F. Fabiano[27,i] , L.N. Falcao[1] , Y. Fan[6] , B. Fang[11,68] ,

L. Fantini[72,p] , M. Faria[43] , S. Farry[54] , D. Fazzini[26,n] , L.F Felkowski[75] , M. Feo[42] ,

M. Fernandez Gomez[40] , A.D. Fernez[60] , F. Ferrari[20] , L. Ferreira Lopes[43] ,

F. Ferreira Rodrigues[2] , S. Ferreres Sole[32] , M. Ferrillo[44] , M. Ferro-Luzzi[42] ,

S. Filippov[38] , R.A. Fini[19] , M. Fiorini[21,j] , M. Firlej[34] , K.M. Fischer[57] ,

D.S. Fitzgerald[78] , C. Fitzpatrick[56] , T. Fiutowski[34] , F. Fleuret[12] , M. Fontana[13] ,

F. Fontanelli[24,l] , R. Forty[42] , D. Foulds-Holt[49] , V. Franco Lima[54] ,

M. Franco Sevilla[60] , M. Frank[42] , E. Franzoso[21,j] , G. Frau[17] , C. Frei[42] ,

D.A. Friday[53] , J. Fu[6] , Q. Fuehring[15] , T. Fulghesu[13] , E. Gabriel[32] , G. Galati[19,g] ,

M.D. Galati[32] , A. Gallas Torreira[40] , D. Galli[20,h] , S. Gambetta[52,42] , Y. Gan[3] ,

M. Gandelman[2] , P. Gandini[25] , Y. Gao[7] , Y. Gao[5] , M. Garau[27,i] ,

L.M. Garcia Martin[50] , P. Garcia Moreno[39] , J. García Pardiñas[26,n] , B. Garcia Plana[40],

F.A. Garcia Rosales[12] , L. Garrido[39] , C. Gaspar[42] , R.E. Geertsema[32] , D. Gerick[17],

L.L. Gerken[15] , E. Gersabeck[56] , M. Gersabeck[56] , T. Gershon[50] , L. Giambastiani[28] ,

V. Gibson[49] , H.K. Giemza[36] , A.L. Gilman[57] , M. Giovannetti[23,t] , A. Gioventù[40] ,

P. Gironella Gironell[39] , C. Giugliano[21,j] , M.A. Giza[35] , K. Gizdov[52] ,

E.L. Gkougkousis[42] , V.V. Gligorov[13,42] , C. Göbel[64] , E. Golobardes[76] ,

D. Golubkov[38] , A. Golutvin[55,38] , A. Gomes[1,2,b,a,†] , S. Gomez Fernandez[39] ,

F. Goncalves Abrantes[57] , M. Goncerz[35] , G. Gong[3] , I.V. Gorelov[38] , C. Gotti[26] ,

J.P. Grabowski[70] , T. Grammatico[13] , L.A. Granado Cardoso[42] , E. Graugés[39] ,

E. Graverini[43] , G. Graziani , A. T. Grecu[37] , L.M. Greeven[32] , N.A. Grieser[59] ,

L. Grillo[53] , S. Gromov[38] , B.R. Gruberg Cazon[57] , C. Gu[3] , M. Guarise[21,j] ,

M. Guittiere[11] , P. A. Günther[17] , E. Gushchin[38] , A. Guth[14] , Y. Guz[38] , T. Gys[42] ,

T. Hadavizadeh[63] , C. Hadjivasiliou[60] , G. Haefeli[43] , C. Haen[42] , J. Haimberger[42] ,

S.C. Haines[49] , T. Halewood-leagas[54] , M.M. Halvorsen[42] , P.M. Hamilton[60] ,

J. Hammerich[54] , Q. Han[7] , X. Han[17] , E.B. Hansen[56] , S. Hansmann-Menzemer[17] ,

L. Hao[6] , N. Harnew[57] , T. Harrison[54] , C. Hasse[42] , M. Hatch[42] , J. He[6,d] ,

K. Heijhoff[32] , F.H Hemmer[42] , C. Henderson[59] , R.D.L. Henderson[63,50] ,

A.M. Hennequin[58] , K. Hennessy[54] , L. Henry[42] , J. Herd[55] , J. Heuel[14] ,

A. Hicheur[2] , D. Hill[43] , M. Hilton[56] , S.E. Hollitt[15] , J. Horswill[56] , R. Hou[7] ,

Y. Hou[8] , J. Hu[17] , J. Hu[66] , W. Hu[5] , X. Hu[3] , W. Huang[6] , X. Huang[68] ,

W. Hulsbergen[32] , R.J. Hunter[50] , M. Hushchyn[38] , D. Hutchcroft[54] , P. Ibis[15] ,

M. Idzik[34] , D. Ilin[38] , P. Ilten[59] , A. Inglessi[38] , A. Iniukhin[38] , A. Ishteev[38] ,

K. Ivshin[38] , R. Jacobsson[42] , H. Jage[14] , S.J. Jaimes Elles[41] , S. Jakobsen[42] ,

E. Jans[32] , B.K. Jashal[41] , A. Jawahery[60] , V. Jevtic[15] , E. Jiang[60] , X. Jiang[4,6] ,

Y. Jiang[6] , M. John[57] , D. Johnson[58] , C.R. Jones[49] , T.P. Jones[50] , B. Jost[42] ,

N. Jurik[42] , I. Juszczak[35] , S. Kandybei[45] , Y. Kang[3] , M. Karacson[42] ,

D. Karpenkov[38] , M. Karpov[38] , J.W. Kautz[59] , F. Keizer[42] , D.M. Keller[62] ,

M. Kenzie[50] , T. Ketel[32] , B. Khanji[15] , A. Kharisova[38] , S. Kholodenko[38] ,

G. Khreich[11] , T. Kirn[14] , V.S. Kirsebom[43] , O. Kitouni[58] , S. Klaver[33] ,

N. Kleijne[29,q] , K. Klimaszewski[36] , M.R. Kmiec[36] , S. Koliiev[46] , L. Kolk[15] ,

A. Kondybayeva[38] , A. Konoplyannikov[38] , P. Kopciewicz[34] , R. Kopecna[17],

P. Koppenburg[32] , M. Korolev[38] , I. Kostiuk[32,46] , O. Kot[46], S. Kotriakhova ,

28

A. Kozachuk[38] , P. Kravchenko[38] , L. Kravchuk[38] , R.D. Krawczyk[42] , M. Kreps[50] ,
S. Kretzschmar[14] , P. Krokovny[38] , W. Krupa[34] , W. Krzemien[36] , J. Kubat[17],
S. Kubis[75] , W. Kucewicz[35] , M. Kucharczyk[35] , V. Kudryavtsev[38] , E.K Kulikova[38] ,
A. Kupsc[77] , D. Lacarrere[42] , G. Lafferty[56] , A. Lai[27] , A. Lampis[27,i] ,
D. Lancierini[44] , C. Landesa Gomez[40] , J.J. Lane[56] , R. Lane[48] , C. Langenbruch[14] ,
J. Langer[15] , O. Lantwin[38] , T. Latham[50] , F. Lazzari[29,r] , M. Lazzaroni[25,m] ,
R. Le Gac[10] , S.H. Lee[78] , R. Lefèvre[9] , A. Leflat[38] , S. Legotin[38] , P. Lenisa[j,21] ,
O. Leroy[10] , T. Lesiak[35] , B. Leverington[17] , A. Li[3] , H. Li[66] , K. Li[7] , P. Li[17] ,
P.-R. Li[67] , S. Li[7] , T. Li[4] , T. Li[66] , Y. Li[4] , Z. Li[62] , X. Liang[62] , C. Lin[6] ,
T. Lin[51] , R. Lindner[42] , V. Lisovskyi[15] , R. Litvinov[27,i] , G. Liu[66] , H. Liu[6] ,
Q. Liu[6] , S. Liu[4,6] , A. Lobo Salvia[39] , A. Loi[27] , R. Lollini[72] , J. Lomba Castro[40] ,
I. Longstaff[53], J.H. Lopes[2] , A. Lopez Huertas[39] , S. López Soliño[40] , G.H. Lovell[49] ,
Y. Lu[4,c] , C. Lucarelli[22,k] , D. Lucchesi[28,o] , S. Luchuk[38] , M. Lucio Martinez[74] ,
V. Lukashenko[32,46] , Y. Luo[3] , A. Lupato[56] , E. Luppi[21,j] , A. Lusiani[29,q] ,
K. Lynch[18] , X.-R. Lyu[6] , R. Ma[6] , S. Maccolini[15] , F. Machefert[11] , F. Maciuc[37] ,
I. Mackay[57] , V. Macko[43] , L.R. Madhan Mohan[48] , A. Maevskiy[38] , D. Maisuzenko[38] ,
M.W. Majewski[34], J.J. Malczewski[35] , S. Malde[57] , B. Malecki[35,42] , A. Malinin[38] ,
T. Maltsev[38] , G. Manca[27,i] , G. Mancinelli[10] , C. Mancuso[11,25,m] ,
R. Manera Escalero[39], D. Manuzzi[20] , C.A. Manzari[44] , D. Marangotto[25,m] ,
J.F. Marchand[8] , U. Marconi[20] , S. Mariani[22,k] , C. Marin Benito[39,42] , J. Marks[17] ,
A.M. Marshall[48] , P.J. Marshall[54], G. Martelli[72,p] , G. Martellotti[30] ,
L. Martinazzoli[42,n] , M. Martinelli[26,n] , D. Martinez Santos[40] , F. Martinez Vidal[41] ,
A. Massafferri[1] , M. Materok[14] , R. Matev[42] , A. Mathad[44] , V. Matiunin[38] ,
C. Matteuzzi[26] , K.R. Mattioli[12] , A. Mauri[32] , E. Maurice[12] , J. Mauricio[39] ,
M. Mazurek[42] , M. McCann[55] , L. Mcconnell[18] , T.H. McGrath[56] , N.T. McHugh[53] ,
A. McNab[56] , R. McNulty[18] , J.V. Mead[54] , B. Meadows[59] , G. Meier[15] ,
D. Melnychuk[36] , S. Meloni[26,n] , M. Merk[32,74] , A. Merli[25,m] , L. Meyer Garcia[2] ,
D. Miao[4,6] , M. Mikhasenko[70,e] , D.A. Milanes[69] , E. Millard[50], M. Milovanovic[42] ,
M.-N. Minard[8,†], A. Minotti[26,n] , T. Miralles[9] , S.E. Mitchell[52] , B. Mitreska[15] ,
D.S. Mitzel[15] , A. Mödden[15] , R.A. Mohammed[57] , R.D. Moise[14] , S. Mokhnenko[38] ,
T. Mombächer[40] , M. Monk[50,63] , I.A. Monroy[69] , S. Monteil[9] , G. Morello[23] ,
M.J. Morello[29,q] , J. Moron[34] , A.B. Morris[42] , A.G. Morris[50] , R. Mountain[62] ,
H. Mu[3] , E. Muhammad[50] , F. Muheim[52] , M. Mulder[73] , K. Müller[44] ,
C.H. Murphy[57] , D. Murray[56] , R. Murta[55] , P. Muzzetto[27,i] , P. Naik[48] ,
T. Nakada[43] , R. Nandakumar[51] , T. Nanut[42] , I. Nasteva[2] , M. Needham[52] ,
N. Neri[25,m] , S. Neubert[70] , N. Neufeld[42] , P. Neustroev[38], R. Newcombe[55],
J. Nicolini[15,11] , D. Nicotra[74] , E.M. Niel[43] , S. Nieswand[14], N. Nikitin[38] ,
N.S. Nolte[58] , C. Normand[8,i,27] , J. Novoa Fernandez[40] , G.N Nowak[59] , C. Nunez[78] ,
A. Oblakowska-Mucha[34] , V. Obraztsov[38] , T. Oeser[14] , D.P. O'Hanlon[48] ,
S. Okamura[21,j] , R. Oldeman[27,i] , F. Oliva[52] , C.J.G. Onderwater[73] , R.H. O'Neil[52] ,
J.M. Otalora Goicochea[2] , T. Ovsiannikova[38] , P. Owen[44] , A. Oyanguren[41] ,
O. Ozcelik[52] , K.O. Padeken[70] , B. Pagare[50] , P.R. Pais[42] , T. Pajero[57] ,
A. Palano[19] , M. Palutan[23] , Y. Pan[56] , G. Panshin[38] , L. Paolucci[50] ,
A. Papanestis[51] , M. Pappagallo[19,g] , L.L. Pappalardo[21,j] , W. Parker[60] , C. Parkes[56] ,
B. Passalacqua[21,j] , G. Passaleva[22] , A. Pastore[19] , M. Patel[55] , C. Patrignani[20,h] ,
C.J. Pawley[74] , A. Pellegrino[32] , M. Pepe Altarelli[42] , S. Perazzini[20] , D. Pereima[38] ,
A. Pereiro Castro[40] , P. Perret[9] , K. Petridis[48] , A. Petrolini[24,l] , A. Petrov[38],
S. Petrucci[52] , M. Petruzzo[25] , H. Pham[62] , A. Philippov[38] , R. Piandani[6] ,
L. Pica[29,q] , M. Piccini[72] , B. Pietrzyk[8] , G. Pietrzyk[11] , M. Pili[57] , D. Pinci[30] ,
F. Pisani[42] , M. Pizzichemi[26,n,42] , V. Placinta[37] , J. Plews[47] , M. Plo Casasus[40] ,

F. Polci[13,42] (iD), M. Poli Lener[23] (iD), A. Poluektov[10] (iD), N. Polukhina[38] (iD), I. Polyakov[42] (iD),
E. Polycarpo[2] (iD), S. Ponce[42] (iD), D. Popov[6,42] (iD), S. Poslavskii[38] (iD), K. Prasanth[35] (iD),
L. Promberger[17] (iD), C. Prouve[40] (iD), V. Pugatch[46] (iD), V. Puill[11] (iD), G. Punzi[29,r] (iD), H.R. Qi[3] (iD),
W. Qian[6] (iD), N. Qin[3] (iD), S. Qu[3] (iD), R. Quagliani[43] (iD), N.V. Raab[18] (iD), B. Rachwal[34] (iD),
J.H. Rademacker[48] (iD), R. Rajagopalan[62], M. Rama[29] (iD), M. Ramos Pernas[50] (iD),
M.S. Rangel[2] (iD), F. Ratnikov[38] (iD), G. Raven[33,42] (iD), M. Rebollo De Miguel[41] (iD), F. Redi[42] (iD),
J. Reich[48] (iD), F. Reiss[56] (iD), C. Remon Alepuz[41], Z. Ren[3] (iD), P.K. Resmi[10] (iD), R. Ribatti[29,q] (iD),
A.M. Ricci[27] (iD), S. Ricciardi[51] (iD), K. Richardson[58] (iD), M. Richardson-Slipper[52] (iD),
K. Rinnert[54] (iD), P. Robbe[11] (iD), G. Robertson[52] (iD), A.B. Rodrigues[43] (iD), E. Rodrigues[54] (iD),
E. Rodriguez Fernandez[40] (iD), J.A. Rodriguez Lopez[69] (iD), E. Rodriguez Rodriguez[40] (iD),
D.L. Rolf[42] (iD), A. Rollings[57] (iD), P. Roloff[42] (iD), V. Romanovskiy[38] (iD), M. Romero Lamas[40] (iD),
A. Romero Vidal[40] (iD), J.D. Roth[78,†], M. Rotondo[23] (iD), M.S. Rudolph[62] (iD), T. Ruf[42] (iD),
R.A. Ruiz Fernandez[40] (iD), J. Ruiz Vidal[41] (iD), A. Ryzhikov[38] (iD), J. Ryzka[34] (iD),
J.J. Saborido Silva[40] (iD), N. Sagidova[38] (iD), N. Sahoo[47] (iD), B. Saitta[27,i] (iD), M. Salomoni[42] (iD),
C. Sanchez Gras[32] (iD), I. Sanderswood[41] (iD), R. Santacesaria[30] (iD), C. Santamarina Rios[40] (iD),
M. Santimaria[23] (iD), E. Santovetti[31,t] (iD), D. Saranin[38] (iD), G. Sarpis[14] (iD), M. Sarpis[70] (iD),
A. Sarti[30] (iD), C. Satriano[30,s] (iD), A. Satta[31] (iD), M. Saur[15] (iD), D. Savrina[38] (iD), H. Sazak[9] (iD),
L.G. Scantlebury Smead[57] (iD), A. Scarabotto[13] (iD), S. Schael[14] (iD), S. Scherl[54] (iD), M. Schiller[53] (iD),
H. Schindler[42] (iD), M. Schmelling[16] (iD), B. Schmidt[42] (iD), S. Schmitt[14] (iD), O. Schneider[43] (iD),
A. Schopper[42] (iD), M. Schubiger[32] (iD), S. Schulte[43] (iD), M.H. Schune[11] (iD), R. Schwemmer[42] (iD),
B. Sciascia[23] (iD), A. Sciuccati[42] (iD), S. Sellam[40] (iD), A. Semennikov[38] (iD), M. Senghi Soares[33] (iD),
A. Sergi[24,l] (iD), N. Serra[44] (iD), L. Sestini[28] (iD), A. Seuthe[15] (iD), Y. Shang[5] (iD), D.M. Shangase[78] (iD),
M. Shapkin[38] (iD), I. Shchemerov[38] (iD), L. Shchutska[43] (iD), T. Shears[54] (iD), L. Shekhtman[38] (iD),
Z. Shen[5] (iD), S. Sheng[4,6] (iD), V. Shevchenko[38] (iD), B. Shi[6] (iD), E.B. Shields[26,n] (iD), Y. Shimizu[11] (iD),
E. Shmanin[38] (iD), R. Shorkin[38] (iD), J.D. Shupperd[62] (iD), B.G. Siddi[21,j] (iD), R. Silva Coutinho[62] (iD),
G. Simi[28] (iD), S. Simone[19,g] (iD), M. Singla[63] (iD), N. Skidmore[56] (iD), R. Skuza[17] (iD),
T. Skwarnicki[62] (iD), M.W. Slater[47] (iD), J.C. Smallwood[57] (iD), J.G. Smeaton[49] (iD), E. Smith[44] (iD),
K. Smith[61] (iD), M. Smith[55] (iD), A. Snoch[32] (iD), L. Soares Lavra[9] (iD), M.D. Sokoloff[59] (iD),
F.J.P. Soler[53] (iD), A. Solomin[38,48] (iD), A. Solovev[38] (iD), I. Solovyev[38] (iD), R. Song[63] (iD),
F.L. Souza De Almeida[2] (iD), B. Souza De Paula[2] (iD), B. Spaan[15,†], E. Spadaro Norella[25,m] (iD),
E. Spedicato[20] (iD), E. Spiridenkov[38], P. Spradlin[53] (iD), V. Sriskaran[42] (iD), F. Stagni[42] (iD),
M. Stahl[42] (iD), S. Stahl[42] (iD), S. Stanislaus[57] (iD), E.N. Stein[42] (iD), O. Steinkamp[44] (iD),
O. Stenyakin[38], H. Stevens[15] (iD), S. Stone[62,†] (iD), D. Strekalina[38] (iD), Y.S Su[6] (iD), F. Suljik[57] (iD),
J. Sun[27] (iD), L. Sun[68] (iD), Y. Sun[60] (iD), P. Svihra[56] (iD), P.N. Swallow[47] (iD), K. Swientek[34] (iD),
A. Szabelski[36] (iD), T. Szumlak[34] (iD), M. Szymanski[42] (iD), Y. Tan[3] (iD), S. Taneja[56] (iD), M.D. Tat[57] (iD),
A. Terentev[38] (iD), F. Teubert[42] (iD), E. Thomas[42] (iD), D.J.D. Thompson[47] (iD), K.A. Thomson[54] (iD),
H. Tilquin[55] (iD), V. Tisserand[9] (iD), S. T'Jampens[8] (iD), M. Tobin[4] (iD), L. Tomassetti[21,j] (iD),
G. Tonani[25,m] (iD), X. Tong[5] (iD), D. Torres Machado[1] (iD), D.Y. Tou[3] (iD), S.M. Trilov[48] (iD),
C. Trippl[43] (iD), G. Tuci[6] (iD), A. Tully[43] (iD), N. Tuning[32] (iD), A. Ukleja[36] (iD), D.J. Unverzagt[17] (iD),
A. Usachov[33] (iD), A. Ustyuzhanin[38] (iD), U. Uwer[17] (iD), A. Vagner[38], V. Vagnoni[20] (iD),
A. Valassi[42] (iD), G. Valenti[20] (iD), N. Valls Canudas[76] (iD), M. Van Dijk[43] (iD), H. Van Hecke[61] (iD),
E. van Herwijnen[55] (iD), C.B. Van Hulse[40,v] (iD), M. van Veghel[73] (iD), R. Vazquez Gomez[39] (iD),
P. Vazquez Regueiro[40] (iD), C. Vázquez Sierra[42] (iD), S. Vecchi[21] (iD), J.J. Velthuis[48] (iD),
M. Veltri[22,u] (iD), A. Venkateswaran[43] (iD), M. Veronesi[32] (iD), M. Vesterinen[50] (iD), D. Vieira[59] (iD),
M. Vieites Diaz[43] (iD), X. Vilasis-Cardona[76] (iD), E. Vilella Figueras[54] (iD), A. Villa[20] (iD),
P. Vincent[13] (iD), F.C. Volle[11] (iD), D. vom Bruch[10] (iD), A. Vorobyev[38], V. Vorobyev[38],
N. Voropaev[38] (iD), K. Vos[74] (iD), C. Vrahas[52] (iD), J. Walsh[29] (iD), G. Wan[5] (iD), C. Wang[17] (iD),
G. Wang[7] (iD), J. Wang[5] (iD), J. Wang[4] (iD), J. Wang[3] (iD), J. Wang[68] (iD), M. Wang[25] (iD), R. Wang[48] (iD),
X. Wang[66] (iD), Y. Wang[7] (iD), Z. Wang[44] (iD), Z. Wang[3] (iD), Z. Wang[6] (iD), J.A. Ward[50,63] (iD),
N.K. Watson[47] (iD), D. Websdale[55] (iD), Y. Wei[5] (iD), B.D.C. Westhenry[48] (iD), D.J. White[56] (iD),

M. Whitehead[53] (iD), A.R. Wiederhold[50] (iD), D. Wiedner[15] (iD), G. Wilkinson[57] (iD),
M.K. Wilkinson[59] (iD), I. Williams[49], M. Williams[58] (iD), M.R.J. Williams[52] (iD), R. Williams[49] (iD),
F.F. Wilson[51] (iD), W. Wislicki[36] (iD), M. Witek[35] (iD), L. Witola[17] (iD), C.P. Wong[61] (iD),
G. Wormser[11] (iD), S.A. Wotton[49] (iD), H. Wu[62] (iD), J. Wu[7] (iD), K. Wyllie[42] (iD), Z. Xiang[6] (iD),
Y. Xie[7] (iD), A. Xu[5] (iD), J. Xu[6] (iD), L. Xu[3] (iD), L. Xu[3] (iD), M. Xu[50] (iD), Q. Xu[6], Z. Xu[9] (iD), Z. Xu[6] (iD),
D. Yang[3] (iD), S. Yang[6] (iD), X. Yang[5] (iD), Y. Yang[6] (iD), Z. Yang[5] (iD), Z. Yang[60] (iD),
L.E. Yeomans[54] (iD), V. Yeroshenko[11] (iD), H. Yeung[56] (iD), H. Yin[7] (iD), J. Yu[65] (iD), X. Yuan[62] (iD),
E. Zaffaroni[43] (iD), M. Zavertyaev[16] (iD), M. Zdybal[35] (iD), O. Zenaiev[42] (iD), M. Zeng[3] (iD),
C. Zhang[5] (iD), D. Zhang[7] (iD), L. Zhang[3] (iD), S. Zhang[65] (iD), S. Zhang[5] (iD), Y. Zhang[5] (iD),
Y. Zhang[57], Y. Zhao[17] (iD), A. Zharkova[38] (iD), A. Zhelezov[17] (iD), Y. Zheng[6] (iD), T. Zhou[5] (iD),
X. Zhou[6] (iD), Y. Zhou[6] (iD), V. Zhovkovska[11] (iD), X. Zhu[3] (iD), X. Zhu[7] (iD), Z. Zhu[6] (iD),
V. Zhukov[14,38] (iD), Q. Zou[4,6] (iD), S. Zucchelli[20,h] (iD), D. Zuliani[28] (iD), G. Zunica[56] (iD).

[1] Centro Brasileiro de Pesquisas Físicas (CBPF), Rio de Janeiro, Brazil
[2] Universidade Federal do Rio de Janeiro (UFRJ), Rio de Janeiro, Brazil
[3] Center for High Energy Physics, Tsinghua University, Beijing, China
[4] Institute Of High Energy Physics (IHEP), Beijing, China
[5] School of Physics State Key Laboratory of Nuclear Physics and Technology, Peking University, Beijing,
China
[6] University of Chinese Academy of Sciences, Beijing, China
[7] Institute of Particle Physics, Central China Normal University, Wuhan, Hubei, China
[8] Université Savoie Mont Blanc, CNRS, IN2P3-LAPP, Annecy, France
[9] Université Clermont Auvergne, CNRS/IN2P3, LPC, Clermont-Ferrand, France
[10] Aix Marseille Univ, CNRS/IN2P3, CPPM, Marseille, France
[11] Université Paris-Saclay, CNRS/IN2P3, IJCLab, Orsay, France
[12] Laboratoire Leprince-Ringuet, CNRS/IN2P3, Ecole Polytechnique, Institut Polytechnique de Paris,
Palaiseau, France
[13] LPNHE, Sorbonne Université, Paris Diderot Sorbonne Paris Cité, CNRS/IN2P3, Paris, France
[14] I. Physikalisches Institut, RWTH Aachen University, Aachen, Germany
[15] Fakultät Physik, Technische Universität Dortmund, Dortmund, Germany
[16] Max-Planck-Institut für Kernphysik (MPIK), Heidelberg, Germany
[17] Physikalisches Institut, Ruprecht-Karls-Universität Heidelberg, Heidelberg, Germany
[18] School of Physics, University College Dublin, Dublin, Ireland
[19] INFN Sezione di Bari, Bari, Italy
[20] INFN Sezione di Bologna, Bologna, Italy
[21] INFN Sezione di Ferrara, Ferrara, Italy
[22] INFN Sezione di Firenze, Firenze, Italy
[23] INFN Laboratori Nazionali di Frascati, Frascati, Italy
[24] INFN Sezione di Genova, Genova, Italy
[25] INFN Sezione di Milano, Milano, Italy
[26] INFN Sezione di Milano-Bicocca, Milano, Italy
[27] INFN Sezione di Cagliari, Monserrato, Italy
[28] Università degli Studi di Padova, Università e INFN, Padova, Padova, Italy
[29] INFN Sezione di Pisa, Pisa, Italy
[30] INFN Sezione di Roma La Sapienza, Roma, Italy
[31] INFN Sezione di Roma Tor Vergata, Roma, Italy
[32] Nikhef National Institute for Subatomic Physics, Amsterdam, Netherlands
[33] Nikhef National Institute for Subatomic Physics and VU University Amsterdam, Amsterdam,
Netherlands
[34] AGH - University of Science and Technology, Faculty of Physics and Applied Computer Science,
Kraków, Poland
[35] Henryk Niewodniczanski Institute of Nuclear Physics Polish Academy of Sciences, Kraków, Poland
[36] National Center for Nuclear Research (NCBJ), Warsaw, Poland
[37] Horia Hulubei National Institute of Physics and Nuclear Engineering, Bucharest-Magurele, Romania
[38] Affiliated with an institute covered by a cooperation agreement with CERN

31

[39] ICCUB, Universitat de Barcelona, Barcelona, Spain

[40] Instituto Galego de Física de Altas Enerxías (IGFAE), Universidade de Santiago de Compostela, Santiago de Compostela, Spain

[41] Instituto de Fisica Corpuscular, Centro Mixto Universidad de Valencia - CSIC, Valencia, Spain

[42] European Organization for Nuclear Research (CERN), Geneva, Switzerland

[43] Institute of Physics, Ecole Polytechnique Fédérale de Lausanne (EPFL), Lausanne, Switzerland

[44] Physik-Institut, Universität Zürich, Zürich, Switzerland

[45] NSC Kharkiv Institute of Physics and Technology (NSC KIPT), Kharkiv, Ukraine

[46] Institute for Nuclear Research of the National Academy of Sciences (KINR), Kyiv, Ukraine

[47] University of Birmingham, Birmingham, United Kingdom

[48] H.H. Wills Physics Laboratory, University of Bristol, Bristol, United Kingdom

[49] Cavendish Laboratory, University of Cambridge, Cambridge, United Kingdom

[50] Department of Physics, University of Warwick, Coventry, United Kingdom

[51] STFC Rutherford Appleton Laboratory, Didcot, United Kingdom

[52] School of Physics and Astronomy, University of Edinburgh, Edinburgh, United Kingdom

[53] School of Physics and Astronomy, University of Glasgow, Glasgow, United Kingdom

[54] Oliver Lodge Laboratory, University of Liverpool, Liverpool, United Kingdom

[55] Imperial College London, London, United Kingdom

[56] Department of Physics and Astronomy, University of Manchester, Manchester, United Kingdom

[57] Department of Physics, University of Oxford, Oxford, United Kingdom

[58] Massachusetts Institute of Technology, Cambridge, MA, United States

[59] University of Cincinnati, Cincinnati, OH, United States

[60] University of Maryland, College Park, MD, United States

[61] Los Alamos National Laboratory (LANL), Los Alamos, NM, United States

[62] Syracuse University, Syracuse, NY, United States

[63] School of Physics and Astronomy, Monash University, Melbourne, Australia, associated to [50]

[64] Pontifícia Universidade Católica do Rio de Janeiro (PUC-Rio), Rio de Janeiro, Brazil, associated to [2]

[65] Physics and Micro Electronic College, Hunan University, Changsha City, China, associated to [7]

[66] Guangdong Provincial Key Laboratory of Nuclear Science, Guangdong-Hong Kong Joint Laboratory of Quantum Matter, Institute of Quantum Matter, South China Normal University, Guangzhou, China, associated to [3]

[67] Lanzhou University, Lanzhou, China, associated to [4]

[68] School of Physics and Technology, Wuhan University, Wuhan, China, associated to [3]

[69] Departamento de Fisica , Universidad Nacional de Colombia, Bogota, Colombia, associated to [13]

[70] Universität Bonn - Helmholtz-Institut für Strahlen und Kernphysik, Bonn, Germany, associated to [17]

[71] Eotvos Lorand University, Budapest, Hungary, associated to [42]

[72] INFN Sezione di Perugia, Perugia, Italy, associated to [21]

[73] Van Swinderen Institute, University of Groningen, Groningen, Netherlands, associated to [32]

[74] Universiteit Maastricht, Maastricht, Netherlands, associated to [32]

[75] Tadeusz Kosciuszko Cracow University of Technology, Cracow, Poland, associated to [35]

[76] DS4DS, La Salle, Universitat Ramon Llull, Barcelona, Spain, associated to [39]

[77] Department of Physics and Astronomy, Uppsala University, Uppsala, Sweden, associated to [53]

[78] University of Michigan, Ann Arbor, MI, United States, associated to [62]

[a] Universidade de Brasília, Brasília, Brazil

[b] Universidade Federal do Triângulo Mineiro (UFTM), Uberaba-MG, Brazil

[c] Central South U., Changsha, China

[d] Hangzhou Institute for Advanced Study, UCAS, Hangzhou, China

[e] Excellence Cluster ORIGINS, Munich, Germany

[f] Universidad Nacional Autónoma de Honduras, Tegucigalpa, Honduras

[g] Università di Bari, Bari, Italy

[h] Università di Bologna, Bologna, Italy

[i] Università di Cagliari, Cagliari, Italy

[j] Università di Ferrara, Ferrara, Italy

[k] Università di Firenze, Firenze, Italy

[l] Università di Genova, Genova, Italy

[m] Università degli Studi di Milano, Milano, Italy

[n] *Università di Milano Bicocca, Milano, Italy*
[o] *Università di Padova, Padova, Italy*
[p] *Università di Perugia, Perugia, Italy*
[q] *Scuola Normale Superiore, Pisa, Italy*
[r] *Università di Pisa, Pisa, Italy*
[s] *Università della Basilicata, Potenza, Italy*
[t] *Università di Roma Tor Vergata, Roma, Italy*
[u] *Università di Urbino, Urbino, Italy*
[v] *Universidad de Alcalá, Alcalá de Henares , Spain*

[†] *Deceased*